tribology in industry

YU ISSN 0354 - 8996
VOLUME 21
SEPTEMBER 1999.
3

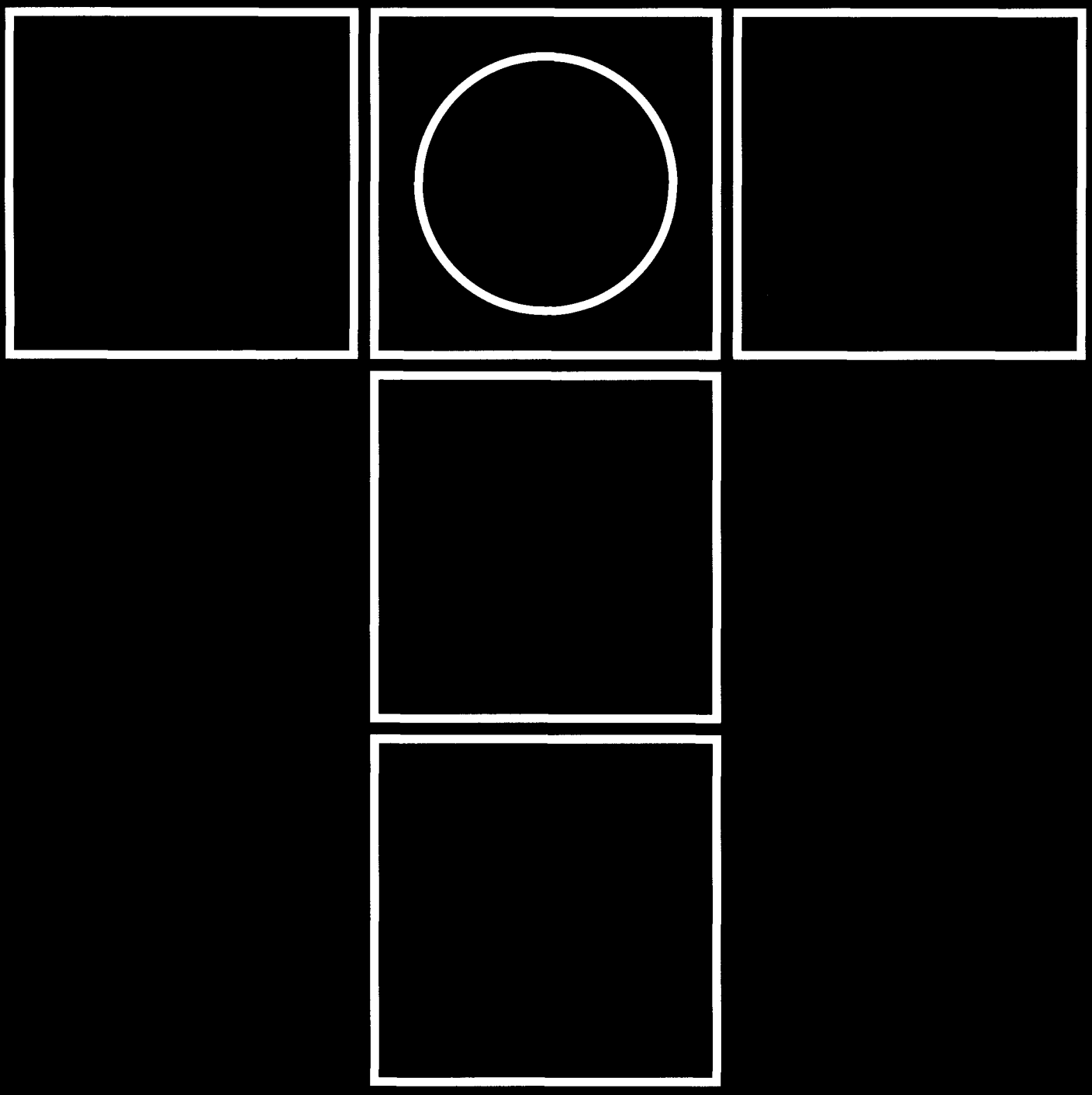

YU ISSN 0354 - 8996

VOLUME 21
N° 3
SEPTEMBER 1999.

tribology in industry

contents

Ancient methods for coatings and surface treatments

"METAL ON METAL"

The gold - and silver plating technique of findings of the ancient graves in Vergina

Professor S. Drougou
Aristoteles University of Thessaloniki, Department of History and Archaeology

1. INTRODUCTION

It was approximately twenty two years ago (1977 - 1978), in the small village of Vergina in northern Pieria, Macedonia, when important tomb paintings date back in 4th century BC, the time of the big glory of Macedonia kingdom, came into light.

The findings were rich and numerous; among them, a lot of impressive metal items (weapons, vases and other equipment items) that place a set of questions not only of archaeological but of technological and metal art interest also.

The objective of my short presentation is basically, to outline certain techniques in metal art, using examples taken from the Vergina findings such as the silver and golden plating of vases; a technique, very popular in the later classic (4th century BC), and Hellenistic times. Of course, special technical issues can not be raised here. Nevertheless, a part of the existing material will be discussed.

2. THE DISCOVERY OF THE ANCIENT TOWN IN VERGINA

Let us have a quick look on the findings first. The big graves found in 1977 and 1978 in Vergina, were proved of significant historical and archaeological importance. They are large underground buildings, normally covered by a tumulus, which in the case of Vergina graves, was substantially large, covering apart from the main tomb construction, other important graves also.

Two large monumental tomb paintings as well as, all the accompanying funeral items were incidentally found inside the tomb. Those items were significant for the personal, private and public life of the dead. The archaeological indications of the excavation, the dating of the monuments, and the funeral items, led the archaeologists to the conclusion that the dead should be identified as a certain historical figure, and admittedly with the Philip II, one of the protagonists of the classical period's historical scene (5th century BC).

A year before that, Prof. M. Andronikos had already identified in the antique city of Vergina, where the Necropolis with the aforementioned grave monuments belonged, the capital of ancient Macedonia, "Aigai". The foundation of this city goes back to the myth and Macedonians cherished it. All Macedonian kings until Alexander the Great were buried there.

Today, at the ancient city Aigai, there is a number of important monuments preserved, such as the famous palace, the ancient theatre, the city walls, as well as two important sanctuaries.

It was therefore expected, that royal graves would be found in the Necropolis of the city Aigai. The discovery of King Philip's grave was more than a happy event among the archaeological research community. At the same time, the rest of the graves into the large Tumulus, had as well been proven of great importance, for various reasons: In almost every one of those monuments, wall paintings of great significance were preserved. These paintings, could be the subject of a whole chapter about the ancient painting of the classical times. The rest of the findings form also with their own characteristics independent chapters in the antique art, e.g. the metal art.

The King Philip's rich tomb gems prominently indicate the wealth and the might of the royal family, representing in a unique way the high level of the art and the technology of that time. Thus giving us quite a representative picture of the classical period in the 4th century BC.

3. THE GOLD - AND SILVER PLATING TECHNIQUE OF THE FINDINGS

The weapons of the deads are works of special luxury and beauty. They were manufactured using various materials, primarily metal, but also wood, ivory and glass. One identifies

the products of an advanced metal art. In almost every case two or more metals were used, while at the same time, details and small surfaces are gold-plated. The valuable shield, a luxurious piece indeed, is made of ivory, glass, gold and silver on a wooden frame. In the centre of the outer side and on the corresponding gold-plated area two ivory figures represent the myth of Achilles and the Amazon queen. A fine thin golden leaf is deposited on a thick layer, whereon the figures are depicted. Little quadratic golden sheets can be seen through the glass in the Meander-pattern. The shield margins consist probably of a mix of gold and silver, while the wide gold stripes of the grip on the inner side of the shield are garnished with relief decoration.

The helmet and the sword regarding their manufacturing technique show a special quality. It is very rare an ancient iron helmet to have survived and the Vergina's exemplar is one of the best preserved and well-known examples. The helmet consists of a number of iron sheets strongly forged and compounded in such a way as to form the round shape of the helmet. This helmet is also decorated with small relief figures. Regarding the sword, various materials had been likewise utilised, mainly natural iron, but also ivory and gold at the grip of the sword, whereon its round surface a tiny gold phoenix is represented.

The iron "thorax" of the dead is a fine piece of forging art. It consists of several thin iron pieces that are connected with hinges so that the thorax width could be adjustable. Finally, it is decorated with small gold ribbons.

The shin-pads belong to the standard armament of a warrior. For the royal dead in the tomb there were several pairs of shin-pads, among them a pair made of gold-plated bronze, a good example of the gilding technique, also known from many other items. One of the most impressive cases is the metal plate of a cooker that consists of a gilded silver sheet (fixed on leather). The plate is decorated with a presentation of the seizure of a town (Troja).

Among the other items in the tomb, the metal vases form a very interesting group of real works of art. They mainly concern symposium vessels, board and drinking vessels, as well as household appliances. As far as the materials are concerned, they were luxurious and finely manufactured, demonstrating the skill and the talent of the ancient craftsmen. The most vases consist of forged silver sheets and have moulded handles and basis. Their details are often gilded.

The bronze lamp-bracket, a real lantern, has a medium size. Its details highlight the differences of the form. The base is high and moulded. The handles are mounted and decorated with one satyr's head each, at their attachment with the body. At the height of these portrayals, a zone surrounds the lantern body with an ivy branch made of silver or, most probably, of silvered bronze, resulting in a beautiful contrast between the white silver and the bronze.

The fine symposium's drinking cups distinguish themselves by their form and especially by their relief details, e.g. the silver drinking cup and the satyr head on the vase bottom are outstanding. Obviously, the Dionysos-follower is already drunk, because he smiles happily. He carries a red braid chaplet and has red beard, which in combination with the gold plating gives a sense of polychrome. The braid strap on the vase exterior is also gilded. The same pattern in a similar technique appears also on a silver wine strainer, whose rim is garnished with a gilded braid strap.

Gold plating, in most of the cases, is the predominant decoration technique. In this discussion, particularly worth mentioning are the ivory figures, which in an impressive frieze decorate a funeral bed. Two such beds were found in a large grave. They were made of wood, clad almost completely with ivory, while the smaller decoration motives are made of glass and gold. On the long side of the furniture there is a frieze with relief figures, which are fixed on a gilded background. The hair and the dresses within these figures are also from gold.

The second Macedonian grave in the big Tumulus, the so-called grave of the "Prince", offers a similar picture. It contains vases, weapons and furniture of similar kinds and forms as the aforementioned grave of Philip. Gilded weapons, gold-ivory beds and silver vases were also found here.

The gilded bronze shin-pads have on their lower rim a narrow zone with gilded palms. The palms at the handles of the silver "Situla" are gilded as well.

The represented pair of the "Dionysos" and the "Maenads" in the ivory frieze of the bed found in the grave of the "Prince" is a fine outstanding work. The gold in the hair of the figures inspires polychrome and plays with the contrast of the red gold and the white yellow combination of the ivory. The rendition of the hair at the head of the grip of a silver "Patera" is very fine also. A large bronze boiler differs from the remaining vases of the grave because of the strange silver plating of its surface. It consists of fine thin silver sheets, which were stuck on the bronze, visible with the naked eye. An iron candelabra that was found in the main grave chamber, a very difficult to preserve piece but nevertheless a very interesting one, was also silvered.

Finally, an example that came into light during this summer (1999) from a recently discovered grave in Vergina; a bronze head belonging to the handles of a big monumental crater. It concerns the figure of the "Dionysos" or probably a "Maenad" with red - blond hair, which is again coated with gold. It remains now the restoration to show the vase their correct picture.

4. CONCLUSIONS

The number of the silvered and gilded findings of Vergina's graves increases every day and outlines a very interesting technique. These findings require however, further physical and chemical, as well as general archaeology-metric investigations, in order to broad our knowledge about the ancient metal art.

According to the ancient gold plating technique the gold sheets were forged between two pieces made of leather or parchment in order to become very thin as shown by recent investigations. The other important question regarding the gold plating technique concerns the adhesive medium used between the substrate and the gold sheet. In the case of the gold plating of clay new investigations came to interesting conclusions and especially that the adhesive medium used contained organic materials and probably substances of eggs. However, the adhesive medium used in the gold plating of metals, is unknown to me, regarding its ingredients.

The investigation of the application of the coatings technique at the vases and the other devices derived from the graves in Vergina is not complete yet. The findings of Vergina became already well known in the international research community. Generally, we have to do with thin silver and gold sheets, which were fixed on the metal surface with the aid of a special organic adhesive medium. At the same time it concerns a widely spread technique of the classical and Hellenistic times in the Greek world, i.e. knowledge and experience from which modern science and archaeology still have much to learn.

RESEARCH

UDK 621.821.5: 62.178.162.4

C. PANDAZARAS, G. PETROPOULOS, G. KOUTLAS

Numerical Modelling of The Behaviour of Various Type Finite Journal Bearings Under Dynamic Loading

The present study draws the results of a developed mathematical model concerning hydrodynamic lubrication in wavy journal bearings of various three dimensional configurations. Reynolds equation of hydrodynamic lubrication is used and solved numerically by carrying out a finite difference approximation scheme (a further developed simulation code [19]) for steady state conditions, as well as when dynamic load is applied during operation while circumferential, axial and combined surface waviness is present in equivalent journal bearing liners. Important conclusions arrived at are: One-wave and two-wave bearings (types of lemon bearings) show better performance than the smooth bearing (lower friction losses) The three-wave bearing didn't appear improved performance in comparison to a circular normal type bearing at any applied load and running regime. In three-wave bearings without axial waviness, increased circumferential wave amplitude leads to minimum lubricant film thickness reduction. High axial waviness amplitude in the case of combined waviness destroys hydrodynamic mechanism.

Key words: Journal bearing, surface macrotopography, fluid film hydrodynamic lubrication, dynamic loading

1. INTRODUCTION

During the last 30 years various theoretical and experimental investigations were carried out regarding unconventional journal bearing configurations behaviour in the case of hydrodynamic lubrication.

The unconventional bearing system characteristics concern either more realistic patterns considering characteristics of machined surfaces as roughness and waviness generating an imperfect circular shape for the journal bearing or generally sliding elements cross sections [3-4], [11], [13], [14-18], [19], [20-21], [27- 31], [33], [34]or recently proposed bearing configurations with specially concepted waved stationary surfaces [6].

In the present paper theoretical results are provided using a further developed calculation code [19], adapted to modelling of hydrodynamic friction mode encountered in wavy shaft - bearing operation in presence of three-dimensional surface irregularities and dynamic loading. These irregularities lead to various geometrical configurations resulting from bearing design, bearing mounting, various journal-bearing manufacturing processes or because of running-in conditions. The three-dimensional variation of fluid lubricant film thickness and hydrodynamic pressure is studied by solving the full Reynolds equation for a smooth model journal-bearing classic type configuration (reference normal type-perfect circular journal bearing cross sections), 1-wave, 2-wave, 3-wave, and multi-wave bearings in presence of circumferential, axial or combined waviness of bearing liner (Fig. 1).

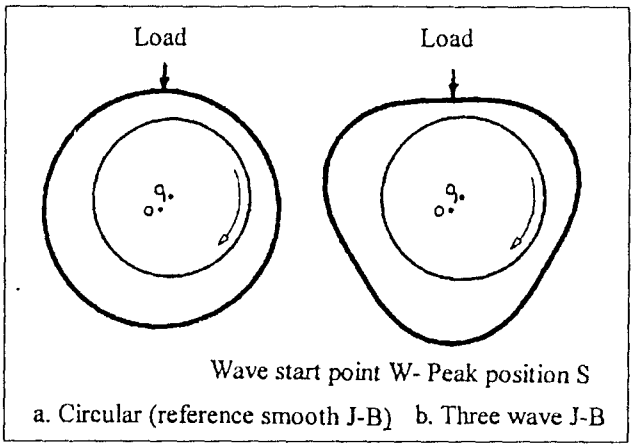

Fig. 1 Schematic cross-sections of Journal-Bearings (J-B) configurations considered.

2. MODEL - DETAILS ON THE SHAFT-BEARING HYDRODYNAMIC FRICTION CODE

2.1. Basic Assumptions

The following parameters are introduced in the three-dimensional code developed:

- Macro-topography of the bearing (bush), axially and circumferentially due to the real shape of the journal bearing (lemon bearing, half lemon bearing, multi-lobe bearing, offset-halves journal bearing known as displaced bearing [29-30], three-wave bearing [6],

C. PANDAZARAS, G. PETROPOULOS, G. KOUTLAS,
Department of Mechanical and Industrial Engineering
University of Thessaly, Pedion Areos,
38334 Volos, Greece

multi-wave bearing, pericycloid bearing, spiral bearing, presence of circumferential, axial or combined waviness form in bearing liner [27]).

- Dynamically alternating load (harmonic or non-harmonic [1], [19], [30]).

In the present work, the basic assumptions made concerning lubricated contact geometry, shaft-bearing relative motion and lubricant characteristics in a shaft-bearing combination are as follows:

Kinematics - Geometry

- The axes of journal and bush are always parallel and the cross-section is perpendicular to them (zero tilt).
- The shaft cross section configuration is perfectly circular.
- No deformation of the shaft-bearing system occurs under hydrodynamic pressure.
- The bearing is floating. The vertical load is applied through the bearing.

Lubrication

- The oil film is sufficient for the hydrodynamic equation to be valid (full average Reynolds equation).
- The lubricating gap is completely filled with the lubricant.
- Lubricant viscosity is constant during the system operation (Newtonian isoviscous fluid).
- The lubricant is incompressible and the flow in the gap of the finite length bearing is laminar.

2.2. INPUT - OUTPUT Parameters

Input: Shaft geometry - diameter D_J, bearing (bush-hole) geometry - diameter D_B and length L_B (total axial, normal to the direction of motion), bearing macro-topography incorporating waviness amplitudes circumferentially (W_c) and axially (W_l) and waviness numbers circumferentially (N_c) and axially (N_l), fluid lubricant viscosity n, shaft rotational speed U, shaft - bearing load function $W(t)$ (Fig.1).

Output: Fluid lubricant film thickness h_{min} - journal center path, shaft eccentricity e, equilibrium angle α measured from West point (clockwise), hydrodynamic pressure p, friction forces (or moments) F_J and F_B, friction coefficient and power losses.

2.3. Principle Of The Model

The purpose of the model is to calculate the load supported by the hydrodynamic fluid lubricant film for given conditions.

The friction force (or moment) is calculated as the sum of the hydrodynamic oil film shearing forces (or moments). It is to be noted that the squeeze term is taken into account in the Reynolds equation.

Thus, the hydrodynamic fluid lubricant film thickness is calculated for a given separation distance of shaft - bearing surfaces. An iterative procedure is then applied in order to calculate the value of the film thickness that yields to the equilibrium between the contact forces and the load acting on the shaft - bearing system.

The hydrodynamic fluid lubricant film thickness is calculated through the well known full Reynolds equation in dimensional or dimensionless form, in polar or rectangular coordinates for the developed surfaces, by adopting the half-Sommerfeld (Gümbel) conditions, $p=0$ in the specified cavitation position. The stretch contribution to load support is neglected.

Reynolds equation is solved numerically by introduction of Nystrom formula into the finite difference iterative method (Gauss-Seidal) for a mesh in 3.6^o and $<1.0\ mm$. The active part of the bearing is meshed in $100x40$ elements. **H**, nodes fluid lubricant film thickness matrix is defined from the real shape of the bearing (Fig. 2), the shape of the shaft and the eccentricity between the shaft and the bearing. **P**, nodes hydrodynamic pressure matrix is formed after solving the Reynolds equation (Fig. 3). The resulting equivalent hydrodynamic force via the computed hydrodynamic pressure must be equal and opposite to the applied bearing-shaft load. When the pressure equations have been satisfied, flow is calculated through the pressure field and the next step is to calculate hydrodynamic friction forces by determining the sum F_H of all the friction components acting on each element of the bearing or the shaft surface.

3. COMPUTATIONAL DATA

Calculations have been carried out for a given nominal geometry. The bearing macro-topography corresponds either to a perfect cylinder or to a multi wavy configuration, in the presence or not of axial waviness. The configuration studied is an optimized Renault journal-bearing (*J-B*) system. This geometry (bearing diameter, bearing length and clearance as well as their dimensionless characteristics) was proposed by the authors for an experimental laboratory simulator under construction providing fluid lubricant film comparative tribological test results under steady state or dynamic loading.

Data used in the code, as well as in the configurations considered are as follows:

Rotational speed N: 1500 - 3000 - 4500 rpm

Geometry: shaft diameter D_J *: 54.746 - 54.766 - 54.806 mm*
bearing diameter D_B *: 54.806 - 54.838 - 54.870 mm*

total J-B length L_B *: 22.420 - 24.420 - 26.420 mm*

Lubricant: absolute viscosity n
(100°C) $= 3.40 \cdot 10^{-3} - 7.42 \cdot 10^{-3} - 11.02 \cdot 10^{-3}$ *Pa.s*

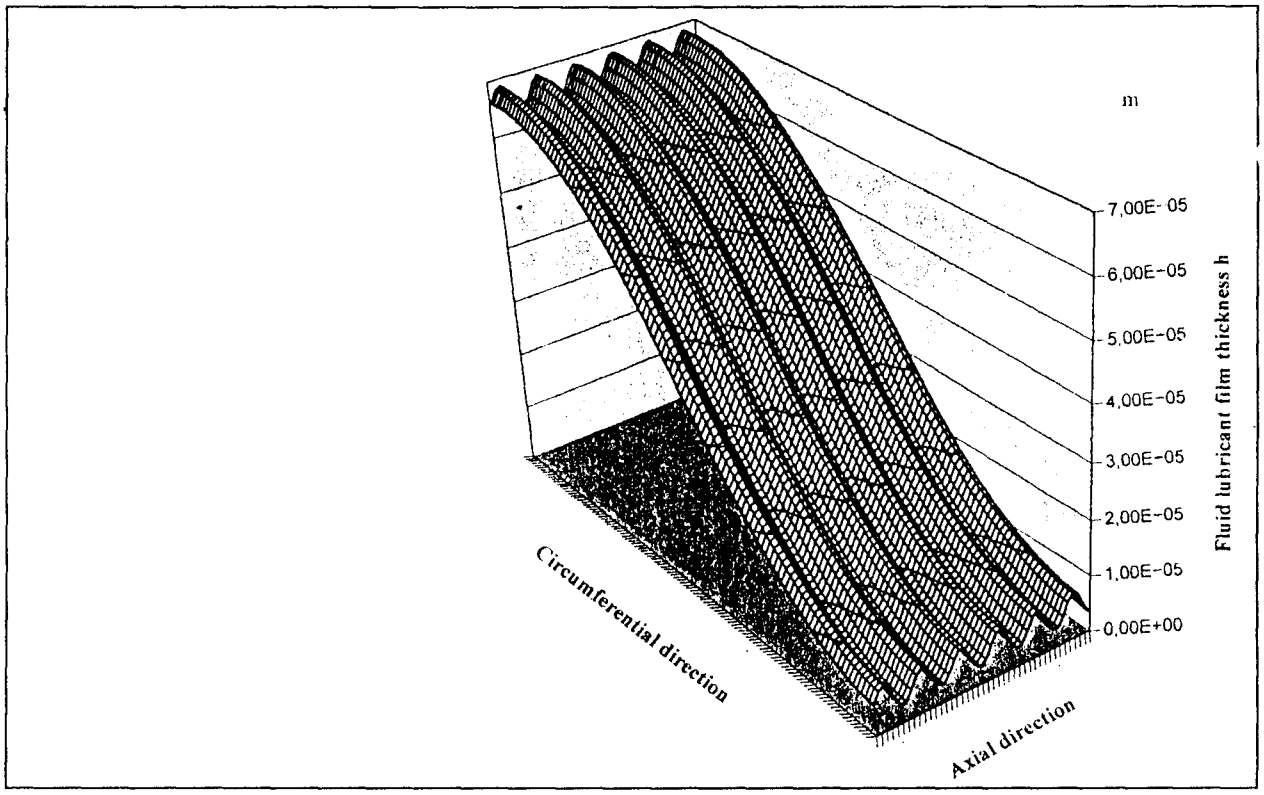

Fig. 2 Fluid lubricant film thickness distribution in the active part of the journal-bearing system under static loading for a combined wavy bearing $N_c=3$, $N_l=5.50$, $W_c=2.50$ m, $W_l=2.50$ m, $n=0.00742$ Pa.s, $N=3000$ rpm

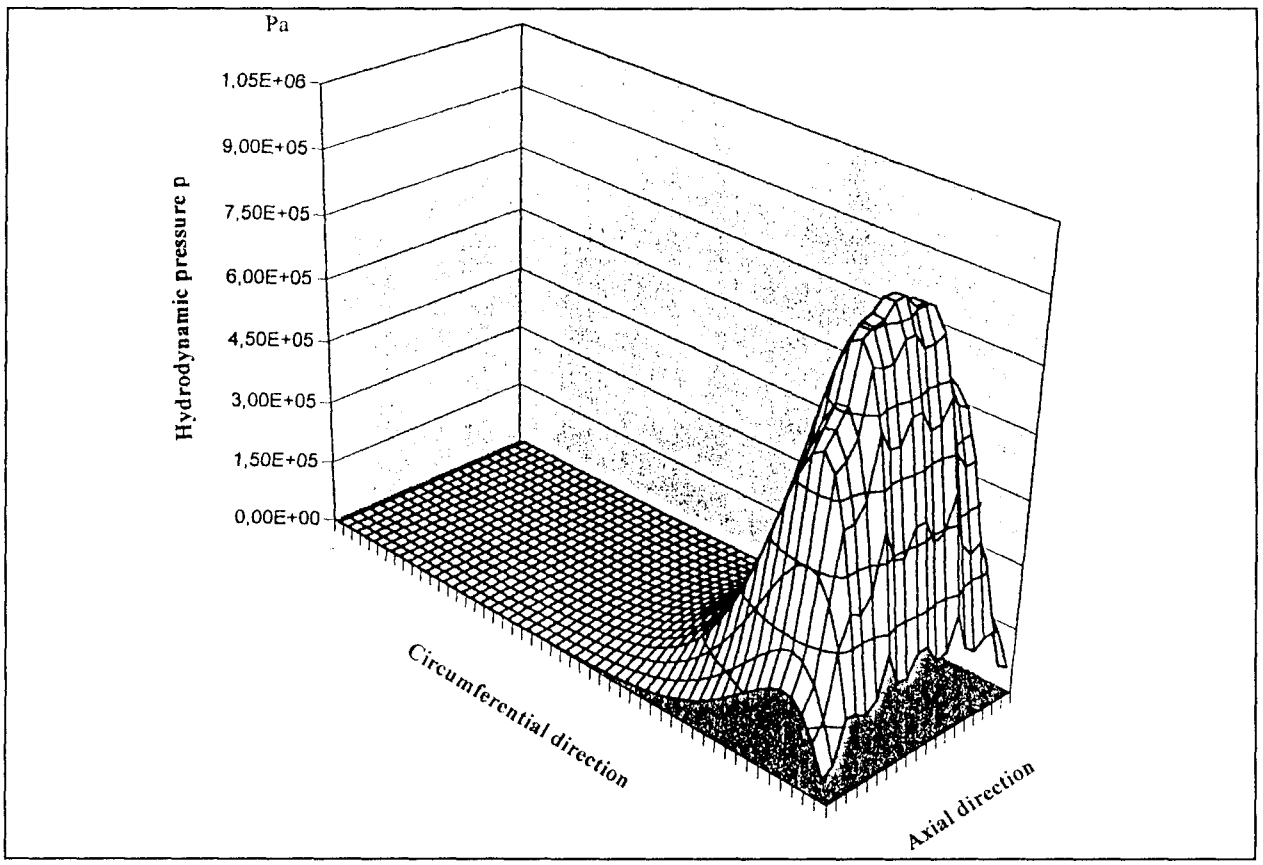

Fig. 3 Hydrodynamic pressure distribution in the active part of the journal-bearing system under static loading for a combined wavy bearing $N_c=3$, $N_l=5.50$, $W_c=2.50$ m, $W_l=2.50$ m, $n=0.00742$ Pa.s, $N=3000$ rpm

Macro-topography: W_c=0.0 to 10.0 μm, W_l=0.0 to 10.0 μm,
N_c=0 to 10, N_l=0 to 10

Load W: *in steady state conditions*
(500)-1500-(2000)-3000-(3500)-4500 N

in vibration conditions
2000 + 1500·cos(ωt) N,
where ω is the shaft angular velocity.

Table 1: Calculated results for smooth journal bearing configuration
n=0.00742 Pa.s, W=3000 N, D_B=54.838 mm, D_J=54.806 mm, L_B=24.420 mm

Rotational speed N [rpm]	Eccentricity e [μm]	Equil. angle α [°]	Mini film thickness h [μm]	Max. Pressure 106[Pa]	Shaft Friction Force [N]	Bearing Friction Force [N]
1500	11.2	136.7	4.80	6.34	5.54	4.98
3000	9.0	145.6	7.00	4.87	11.43	11.04
4500	7.6	151.0	8.40	4.34	17.77	17.46

D_J=54.766 mm

Rotation speed N [rpm]	Eccentricity e [μm]	Equil. angle α [°]	Mini film thickness h [μm]	Max. Pressure 106[Pa]	Shaft Friction Force [N]	Bearing Friction Force [N]
1500	32.2	121.7	3.80	10.76	3.31	0.98
3000	29.9	127.0	6.10	8.68	5.32	3.50
4500	28.0	131.1	8.00	7.38	7.53	6.00

D_J=54.746 mm

Rotation speed N [rpm]	Eccentricity e [μm]	Equil. angle α [°]	Mini film thick-ness h [μm]	Max. Pressure 106[Pa]	Shaft Friction Force [N]	Bearing Friction Force [N]
1500	42.7	117.0	3.26	13.20	3.58	2.67
3000	40.4	122.0	5.56	10.20	4.79	1.97

Table 2: Calculated results for One-Wave Bearing (peak position N)
n=0.00742 Pa.s, N= 3000 rpm, W=3000 N, W_l=0.0 μm

W_c Wave amplitude [μm]	Eccentricity e [μm]	Equil. angle α [°]	Mini film thick-ness h [μm]	Max. Pressure 10^6[Pa]	Shaft Friction Force [N]	Bearing Friction Force [N]
0.00	29.90	127.00	6.10	8.68	5.32	3.50
1.00	30.72	126.97	6.15	8.70	5.26	3.44
2.50	32.05	126.70	6.14	8.72	5.20	3.32
5.00	34.25	126.20	6.13	8.90	5.08	3.12
10.00	38.65	125.33	6.10	9.17	4.89	2.77
15.00	43.05	124.60	6.05	9.46	4.74	2.45

Table 3: Calculated results for One-Wave Bearing (peak position N)
n=0.00742 Pa.s, N= 3000 rpm, W=3000 N, N_l=4.5

W_c/W_l Wave amplitude [μm]	Eccentricity e [μm]	Equil. angle α [°]	Mini film thick-ness h [μm]	Max. Pressure 10^6[Pa]	Shaft Friction Force [N]	Bearing Friction Force [N]
0.0/0.0	29.90	127.00	6.10	8.68	5.32	3.50
0.0/5.0	29.60	128.40	1.40	8.43	5.30	3.51
5.0/0.0	34.25	126.20	6.13	8.90	5.08	3.12
5.0/5.0	34.02	127.40	1.35	8.77	5.04	3.13
10.0/0.0	38.65	125.30	6.10	9.17	4.89	2.77

The ***reference smooth journal bearing configuration*** considered in the present paper has the following characteristics:

shaft diameter D_J: *54.766 mm*
bearing diameter D_B: *54.838 mm*
total J-B length L_B: *24.420 mm*

The ***reference operational conditions*** are as follows:

Rotational speed N: *3000 rpm*

Lubricant: *absolute viscosity n (100°C) = 7.42·10-3 Pa.s*

Load W: *in steady state conditions 3000 N*

Table 4: Calculated results for Two-Wave Bearing reference configuration (peak position NW-SE)
n=0.00742 Pa.s, N= 3000 rpm, W=3000 N, W_l=0.0 μm

Wc Wave amplitude [μm]	Eccentricity e [μm]	Equil. angle α [°]	Mini film thickness h [μm]	Max. Pressure 10^6[Pa]	Shaft Friction Force [N]	Bearing Friction Force [N]
0	29.90	127.00	6.10	8.68	5.32	3.50
1.00	30.80	126.50	6.03	8.76	5.27	3.39
2.50	32.22	125.50	5.85	9.06	5.22	3.19
5.00	34.60	124.03	5.56	9.62	5.18	2.85
10.00	39.28	121.50	5.05	10.63	5.17	2.19
15.00	43.95	119.30	4.53	11.83	5.35	1.45

Table 5: Calculated results for Two-Wave Bearing reference configuration (peak position W-E)
n=0.00742 Pa.s, N= 3000 rpm, W=3000 N, W_l=0.0 μm

Wc Wave amplitude [μm]	Eccentricity e [μm]	Equil. angle α [°]	Mini film thickness h [μm]	Max. Pressure 10^6[Pa]	Shaft Friction Force [N]	Bearing Friction Force [N]
0	29.90	127.00	6.10	8.68	5.32	3.50
1.00	30.83	127.07	6.15	8.58	5.28	3.48
2.50	32.28	126.92	6.17	8.60	5.25	3.43
5.00	34.72	126.64	6.17	8.73	5.19	3.33
10.00	39.60	126.20	6.17	8.91	5.08	3.15
15.00	44.45	125.73	6.19	9.02	4.97	2.99

Table 6: Calculated results for Two-Wave Bearing (peak position NW-SE)
n=0.00742 Pa.s, N= 3000 rpm, W=3000 N, N_l=4.5

Wc/Wl Wave amplitude [μm]	Eccentricity e [μm]	Equil. angle α [°]	Mini film thickness h [μm]	Max. Pressure 10^6[Pa]	Shaft Friction Force [N]	Bearing Friction Force [N]
0.0/0.0	29.90	127.00	6.10	8.68	5.32	3.50
0.0/5.0	29.60	128.40	1.40	8.43	5.30	3.51
5.0/0.0	34.60	124.00	5.56	9.62	5.18	2.85
5.0/5.0	34.45	125.00	0.71	9.52	5.42	2.57
10.0/0.0	39.28	121.50	5.05	10.63	5.17	2.19
10.0/5.0	39.18	121.90	0.15	21.60	6.26	1.06

Table 7: Calculated results for Two-Wave Bearing (peak position W-E)
n=0.00742 Pa.s, N= 3000 rpm, W=3000 N, N_l=4.5

W_c/W_l Wave amplitude [μm]	Eccentricity e [μm]	Equil. angle α[°]	Mini film thickness h [μm]	Max. Pressure 10^6[Pa]	Shaft Friction Force [N]	Bearing Friction Force [N]
0.0/0.0	29.90	127.00	6.10	8.68	5.32	3.50
0.0/5.0	29.60	128.40	1.40	8.43	5.30	3.51
5.0/0.0	34.72	126.60	6.17	8.73	5.19	3.33
5.0/5.0	27.52	125.70	0.71	9.52	5.42	2.57
10.0/0.0	39.60	126.20	6.17	8.91	5.08	3.15
10.0/5.0	25.35	123.00	0.12	23.64	6.48	1.54

4. COMMENTS - CONCLUSIONS

In a previous work [19]a real lemon bearing was studied in terms of a mounting effect of the two part nominally cylindrical journal-bearing geometry. In the present study waviness is considered as geometrical deviation caused by the interaction of machining process and machine tool systems. A corresponding evaluation and analysis of its characteristics could seriously contribute in the direction of tribosystem optimization. A basis is created towards a new improved detailed analysis of the performance concerning wavy journal-bearing functional behaviour.

4.1. Smooth Bearing Behaviour

As the first step, a journal-bearing configuration of a perfect and smooth cylindrical form is studied. Smooth journal-bearing geometry is always considered as the ideal and reference configuration for comparison with the various ones that represent geometrical deviations (Table 1).

4.2. Wavy Bearing Behaviour

The second step is the study of wavy bearings operational behaviour. The proposed algorithmic scheme for calculating contact geometry and friction between shaft and

Table 8: Comparison between NASA measured-calculated results for Three-Wave Gas Lubricated Bearing [6] (peak position S) and calculated results for very low viscosity incompressible lubricant ($n=0.004 \cdot 10^{-3}$ Pa.s) $D_B=51.117$ mm, $D_J=51.091$ mm, $L_B=58.00$ mm, $W_c=7.25$ μm, $W_l=0.0$ μm

Rotation. Speed N [rpm]	Bearing Load [N]	NASA Meas. e [μm]	NASA Calcul. e [μm]	Model e [μm]	NASA Meas. a [°]	NASA Calcul. a [°]	Model A [°]
5261	57.85	8.070	10.074	8.000	143.97	157.40	136.40
5258	71.20	8.374	10.687	8.775	142.20	156.50	134.60
10012	66.75	4.293	7.124	5.920	138.54	155.20	138.00
10081	137.95	9.434	9.720	8.810	135.36	144.00	134.70
15058	151.30	7.235	8.157	7.650	131.61	141.90	137.10
15089	249.20	10.202	10.201	9.440	136.11	138.20	132.70
15091	262.55	10.335	10.288	9.600	132.69	137.80	132.20

Table 9: Calculated results for Three-Wave Bearing (peak position S) $n=0.00742$ Pa.s, $N=3000$ rpm, $W=3000$ N, $W_l=0.0$ μm

Wave amplitude [μm]	Eccentricity e [μm]	Equil. angle α [°]	Mini film thickness h [μm]	Max. Pressure 10^6[Pa]	Shaft Friction Force [N]	Bearing Friction Force [N]
0.00	29.90	127.00	6.10	8.68	5.32	3.50
1.00	30.00	126.70	5.90	8.90	5.32	3.39
2.50	30.22	124.42	5.54	9.47	5.36	3.18
5.00	30.55	122.06	4.98	10.45	5.48	2.80
10.00	31.10	118.13	3.96	12.66	6.04	1.79
15.00	31.50	114.94	3.09	15.25	7.08	0.36

Table 10: Calculated results for Three-Wave Bearing (peak position S) $n=0.00742$ Pa.s, $N=3000$ rpm, $W=3000$ N, $N_l=5.50$

W_c/W_l Wave amplitude [μm]	Eccentricity e [μm]	Equil. angle α [°]	Mini film thickness h [μm]	Max. Pressure 10^6[Pa]	Shaft Friction Force [N]	Bearing Friction Force [N]
0.0/0.0	29.90	127.00	6.10	8.68	5.32	3.50
0.0/2.5	29.87	127.42	3.62	8.75	5.28	3.51
0.0/5.0	29.60	128.00	1.40	8.43	5.29	3.50
2.5/0.0	30.22	124.42	5.54	9.47	5.36	3.18
5.0/0.0	30.55	122.06	4.98	10.45	5.48	2.80
10.0/0.0	31.10	118.10	3.96	12.66	6.04	1.79
2.5/2.5	30.28	124.72	2.99	9.66	5.34	3.16
5.0/5.0	30.40	122.63	0.13	23.10	6.53	1.71
10.0/5.0	30.74	116.82	Contact*	-	-	-

Table 11: Calculated results for Multi-Wave Bearing (start point W)
n=0.00742 Pa.s, N= 3000 rpm, W=3000 N, W_c=2.5 μm, W_l=0.0 μm

Wave number N_c	Eccentricity e [μm]	Equil. angle α [°]	Mini film thickness h [μm]	Max. Pressure 10^6[Pa]	Shaft Friction Force [N]	Bearing Friction Force [N]
0	29.90	127.00	6.10	8.68	5.32	3.50,
1	32.05	126.70	6.14	8.72	5.20	3.32
2	32.22	125.50	5.85	9.06	5.22	3.19
3	30.22	124.42	5.54	9.47	5.36	3.18
4	27.95	124.98	5.74	9.21	5.37	3.38
5	27.48	127.84	6.48	8.36	5.20	3.59
6	29.07	131.67	6.95	7.52	5.06	3.60
7	31.30	132.70	6.99	6.94	5.08	3.41
8	32.03	128.82	5.76	7.89	5.39	3.08
9	30.55	123.93	4.75	10.40	5.80	2.88
10	28.60	122.14	4.95	11.21	5.71	3.22

Table 12: Calculated results for Multi-Wave Bearing (start point W) n=0.00742 Pa.s, N= 3000 rpm, W=3000 N, W_c=2.50 μm, W_l=2.50 μm, N_l=3.50

Wave number N_c	Eccentricity e [μm]	Equil. angle α [°]	Mini film thickness h [μm]	Max. Pressure 10^6[Pa]	Shaft Friction Force [N]	Bearing Friction Force [N]
0	30.10	127.02	3.40	9.15	5.30	3.47
1	32.30	126.56	3.39	9.31	5.17	3.27
2	32.48	125.42	3.10	9.64	5.22	3.13
3	30.48	124.28	2.79	10.14	5.38	3.11
4	28.20	124.90	2.99	9.85	5.37	3.32
5	27.70	127.80	3.75	8.87	5.18	3.56
6	29.30	131.44	4.23	8.05	5.03	3.57
7	31.50	132.51	4.29	7.39	5.06	3.38
8	32.25	128.70	3.03	8.33	5.40	3.03
9	30.80	123.73	2.00	11.30	5.91	2.71
10	28.85	122.02	2.20	12.35	5.76	3.11

Table 13: Calculated results for Three-Wave Bearing (peak position S)
n=0.00742 Pa.s, N= 3000 rpm, W=3000 N, W_c=2.5 μm, N_c=3, W_l=2.5 μm

Wave number N_c	Eccentricity e [μm]	Equil. angle α [°]	Mini film thickness h [μm]	Max. Pressure 10^6[Pa]	Shaft Friction Force [N]	Bearing Friction Force [N]
0	30.22	124.42	5.54	9.47	5.36	3.18
-0.5	28.85	123.98	4.41	11.27	5.55	3.38
+0.5	31.45	124.87	4.12	8.13	5.20	3.02,
-1.5	29.50	125.82	3.77	8.07	5.39	3.33
+1.5	30.80	122.93	2.46	14.42	5.49	2.93
-2.5	29.70	125.60	3.56	8.82	5.36	3.29
+2.5	30.60	123.89	2.66	10.35	5.41	3.06
-3.5	29.80	125.47	3.47	8.54	5.35	3.29
+3.5	30.48	124.28	2.79	10.15	5.38	3.11
-4.5	29.90	125.32	3.39	8.72	5.33	3.27
+4.5	30.38	124.54	2.95	9.64	5.36	3.17

- means that bearing longitudinal waviness has initially positive values so that oil film thickness possesses lower starting values with regard to the mean surfaces separation value.
+means that bearing longitudinal waviness has initially negative values so that oil film thickness possesses higher starting values with regard to the mean surfaces separation value (Fig. 1).

bearing under steady-state conditions, as well as under dynamic load supports the following conclusions:

Minimum wear should take place when the minimum fluid lubricant film thickness increases. Minimum friction losses appear in the minimum film region with low viscosity, low speed, low load, high clearance and small bearing length. In this case maximum hydrodynamic pressure increases, as well as its spatial derivative (dp/dz) value.

Lubrication regime is not fully hydrodynamic, if roughness is taken into account. Hydrodynamic shaft - bearing friction losses are essentially low. This last point is in agreement with results found by various authors ($\mu < 0.005$) [2]. For low waviness amplitude the half of the journal-bearing peripheral lubricated length is practically inactive.

The wavy bearing performance is dependent upon the waves amplitude and waviness numbers.

One-wave (Tables 2-3) and two-wave bearings (types of lemon bearings) (Tables 4-7) exhibit better performance than the smooth bearing (lower friction losses) with higher surfaces separation distance values, if there is no limitation in journal operational eccentricity values of the journal.

Table 14: Calculated results for Smooth Bearing Steady state loading conditions $n=0.00742$ Pa.s, $N=3000$ rpm

Load W [N]	Eccentricity e [μm]	Equil. angle α [°]	Mini film thickness h [μm]	Max. Pressure 10^6[Pa]	Shaft Friction Force [N]	Bearing Friction Force [N]
500	18.88	148.00	17.12	0.76	5.15	5.02
1500	26.49	134.05	9.50	3.35	4.93	4.26
2000	28.03	131.12	7.98	4.96	5.02	4.00
3000	29.90	127.00	6.10	8.68	5.32	3.50
3500	30.45	125.78	5.55	10.50	5.49	3.28
4500	31.39	134.40	4.60	14.97	5.94	2.72

Table 15: Calculated results for Smooth Bearing Dynamic load $W=2000+1500\cdot\sin(\omega t)$, $n=0.00742$ Pa.s, $N=3000$ rpm

Load W [N]	Eccentricity e [μm]	Equil. angle α [°]	Mini film thickness h [μm]	Max. Pressure 10^6[Pa]	Shaft Friction Force [N]	Bearing Friction Force [N]
2000	28.35	129.53	7.65	5.13	5.02	3.97
3060	29.90	127.00	6.10	8.75	5.33	3.50
3500	30.42	125.84	5.58	10.43	5.48	3.29
3060	29.95	126.98	6.06	8.79	5.33	3.49
2000	28.08	131.08	7.93	4.99	5.00	4.00
940	23.73	139.71	12.28	1.80	4.93	4.59
500	19.00	148.30	16.70	0.76	5.14	5.01
940	23.52	139.64	12.48	1.80	4.95	4.60
2000	27.96	131.14	8.04	4.96	5.00	4.10
3060	29.90	127.00	6.11	8.74	5.33	3.50
3500	30.43	125.85	5.58	10.43	5.49	3.29
3060	29.95	126.98	6.06	8.79	5.33	3.49

Table 16: Calculated results for One-Wave Bearing (peak position N) Steady state loading conditions $n=0.00742$ Pa.s, $N=3000$ rpm $N_c=1$, $N_l=5.50$, $W_c=2.50$ μm, $W_l=2.50$ μm

Load W [N]	Eccentricity e [μm]	Equil. angle α [°]	Mini film thickness h [μm]	Max. Pressure 10^6[Pa]	Shaft Friction Force [N]	Bearing Friction Force [N]
500	22.13	149.89	13.57	0.99	4.77	4.61
1500	30.18	136.40	5.52	4.58	4.67	3.77
2000	31.73	133.40	3.97	6.80	4.82	3.46
3000	33.58	129.37	2.12	11.90	5.31	2.79
3500	34.18	127.91	1.52	14.93	5.34	2.41
4500	35.03	125.52	0.67	25.17	6.59	1.38

For one-wave bearing (North peak position) without axial waviness an increase of circumferential wave amplitude leads to insignificant decrease of the minimum fluid lubricant film thickness value and to reduction of journal friction losses (Table 2). The presence of axial waviness in the case of one-wave bearing can reduce journal friction losses, even if the minimum film thickness decreases significantly (Table 3). For two-wave (NW-SE peak posi-

Table 17: Calculated results for One-Wave Bearing (peak position N) Dynamic load $W= 2000+1500\cdot\sin(\omega t)$, $n=0.00742$ Pa.s, $N= 3000$ rpm $N_c=1$, $N_l=5.50$, $W_c=2.50$ μm, $W_l=2.50$ μm

Load W [N]	Eccentricity e [μm]	Equil. angle α [°]	Mini film thickness h [μm]	Max. Pressure 10^6[Pa]	Shaft Friction Force [N]	Bearing Friction Force [N]
2000	31.95	131.93	3.74	7.02	4.84	3.43
3060	33.63	129.26	2.07	12.16	5.34	2.76
3500	34.15	127.99	1.55	14.77	5.62	2.43
3060	33.65	129.22	2.04	12.23	5.35	2.75
2000	31.75	133.38	3.95	6.82	4.83	3.46
940	27.23	141.83	8.47	2.40	4.60	4.16
500	22.23	150.12	13.46	0.99	4.77	4.60
940	27.11	141.80	8.58	2.41	4.61	4.17
2000	31.69	133.42	4.08	6.81	4.83	3.46
3060	33.62	129.25	2.07	12.16	5.34,	
3500	34.14	128.03	1.55	14.72	5.61	2.44
3060	33.65	129.22	2.04	12.23	5.35	2.75

Table 18: Calculated results for Two-Wave Bearing (peak position NW-SE) Steady state loading conditions $n=0.00742$ Pa.s, $N= 3000$ rpm $Nc=2$, $N_l=5.50$, $W_c=2.50$ μm, $W_l=2.50$ μm

Load W [N]	Eccentricity e [μm]	Equil. angle α [°]	Mini film thickness h [μm]	Max. Pressure 10^6[Pa]	Shaft Friction Force [N]	Bearing Friction Force [N]
500	22.48	148.31	13.10	1.04	4.71	4.54
1500	30.48	135.24	5.10	4.75	4.65	3.70
2000	32.00	132.30	3.58	7.10	4.83	3.36
3000	33.83	128.27	1.75	12.50	5.42	2.59
3500	34.40	126.80	1.18	16.11	5.85	2.11
4500	35.23	124.22	0.36	38.08	7.68	2.07

Table 19: Calculated results for Two-Wave Bearing (peak position NW-SE) Dynamic load $W= 2000+1500\cdot\sin(\omega\mu t)$, $n=0.00742$ Pa.s, $N= 3000$ rpm $N_c=2$, $N_l=5.50$, $W_c=2.50$ μm, $W_l=2.50$ μm

Load W [N]	Eccentricity e [μm]	Equil. angle α [°]	Mini film thickness h [μm]	Max. Pressure 10^6[Pa]	Shaft Friction Force [N]	Bearing Friction Force [N]
2000	32.23	130.84	3.35	7.30	4.85	3.32
3060	33.38	128.15	1.70	12.77	5.45	2.56
3500	34.38	126.90	1.20	15.90	5.83	2.13
3060	33.90	128.10	1.68	12.82	5.46	2.55
2000	32.03	132.27	3.56	7.11	4.83	3.35
940	27.55	140.56	8.03	2.49	4.56	4.09
500	22.55	148.57	13.03	1.04	4.70	4.53
940	27.42	140.54	8.15	2.49	4.57	4.10
2000	31.98	132.31	3.61	7.11	4.83	3.36
3060	33.88	128.15	1.70	12.77	5.46	2.56
3500	34.38	126.90	1.20	15.90	5.83	2.13
3060	33.90	128.10	1.68	12.82	5.46	2.55

tion) this effect takes place for limited values of wave amplitude (Table 6). On the other hand, for a W-E peak orientation the increase of the circumferential wave amplitude leads to increase in the minimum fluid lubricant film thickness value and decreases friction losses (Table 7). The presence of low amplitude axial waviness in the case of two-wave bearing can reduce journal friction losses, even if the minimum film thickness lessens significantly. The three-wave bearing didn't appear to have improved performance in comparison to a circular normal bearing at any applied load and functioning regime. For this type of bearing without axial waviness, when the circumferential wave amplitude increases, the minimum film thickness decreases, consequently increasing journal friction losses. Under steady-state conditions the 3-wave bearing seems to have similar behaviour to its smooth equivalent one operating with a lower absolute viscosity of the fluid lubricant. Calculation code tested on the NASA 3-wave model bearing [6]for an incompressible fluid lubricant of very low viscosity provided similar results (Table 8).

4.3. Concluding Remarks

Every wavy bearing behaviour during operation with smooth journal depends on the load direction and the wave location. Especially for wavy bearing configurations with low circumferential wave numbers the wave peak orientation is significant. Shaft-bearing relative position is very sensitive to wave position-orientation. For multi-wave bearing the last remark in not suggested to be important and the wave start point position may not be considered.

Increasing the circumferential waviness number of the multi-wavy bearing a variation of the minimum fluid lubricant film thickness appears with significant relevant variation of the friction losses. Thus, for circumferential waviness numbers N_c 1-2 and 6-7 an increase of minimum film thickness as well as a decrease of friction losses is observed (Table 11). This fact is noted also for a combined circumferential-axial waviness (Table 12-Fig.4).

Anti-diametrical wave peak configurations corresponding to the smooth bearing behaviour indices are nearly

Table 20: Calculated results for Three-Wave Bearing (peak position S) Steady state loading conditions $n=0.00742$ Pa.s, $N=3000$ rpm $Nc=3$, $N_l=5.50$, $W_c=2.50$ μm, $W_l=2.50$ μm

Load W [N]	Eccentricity e [μm]	Equil. angle α [°]	Mini film thickness h [μm]	Max. Pressure 10^6[Pa]	Shaft Friction Force [N]	Bearing Friction Force [N]
500	20.70	146.78	12.56	1.09	4.79	4.62
1500	28.60	134.20	4.66	4.96	4.74	3.75
2000	30.10	131.27	3.17	7.34	4.94	3.39
3000	31.88	127.27	1.39	13.28	5.67	2.49
3500	32.45	125.67	0.82	19.85	6.36	1.74
4500	33.20	122.88	0.07	96.30	10.09	2.06

Table 21: Calculated results for Three-Wave Bearing (peak position S) Dynamic load $W=2000+1500\cdot\sin(\omega t)$, $n=0.00742$ Pa.s, $N=3000$ rpm $N_c=3$, $N_l=5.50$, $W_c=2.50$ μm, $W_l=2.50$ μm

Load W [N]	Eccentricity e [μm]	Equil. angle α [°]	Mini film thickness h [μm]	Max. Pressure 10^6[Pa]	Shaft Friction Force [N]	Bearing Friction Force [N]
2000	30.30	129.82	2.96	7.56	4.96	3.35
3060	31.93	127.15	1.34	13.68	5.71	2.43
3500	32.43	125.77	0.84	19.30	6.31	1.79
3060	31.95	127.06	1.32	13.80	5.73	2.42
2000	30.13	131.25	3.14	7.36	4.94	3.38
940	25.70	139.41	7.56	2.59	4.64	4.16
500	20.78	147.05	12.49	1.08	4.79	4.62
940	25.58	139.42	7.69	2.58	4.65	4.17
2000	30.08	131.29	3.19	7.36	4.94	3.39
3060	31.93	127.13	1.34	13.68	5.71	2.43
3500	32.43	125.76	0.84	19.30	6.31	1.79
3060	31.95	127.06	1.32	13.80	5.73	2.42

symmetric and centered on the nominal smooth bearing operational points.

Monotony is probably not indicated in the relationship between the circumferential waviness number and journal bearing operational behaviour magnitudes: as journal bearing eccentricity, equilibrium angle, minimum film thickness value and friction losses (Tables 11 and 12-Fig.4).

High axial waviness amplitude in the case of combined waviness destroys hydrodynamic mechanism by decreasing oil minimum film thickness (Tables 10-13). High values of axial waviness number provide the best results concerning minimum film thickness and journal friction losses. Rotating and alternating loads causing journal center paths (closed orbits) does not seem to be more critical than static loads.

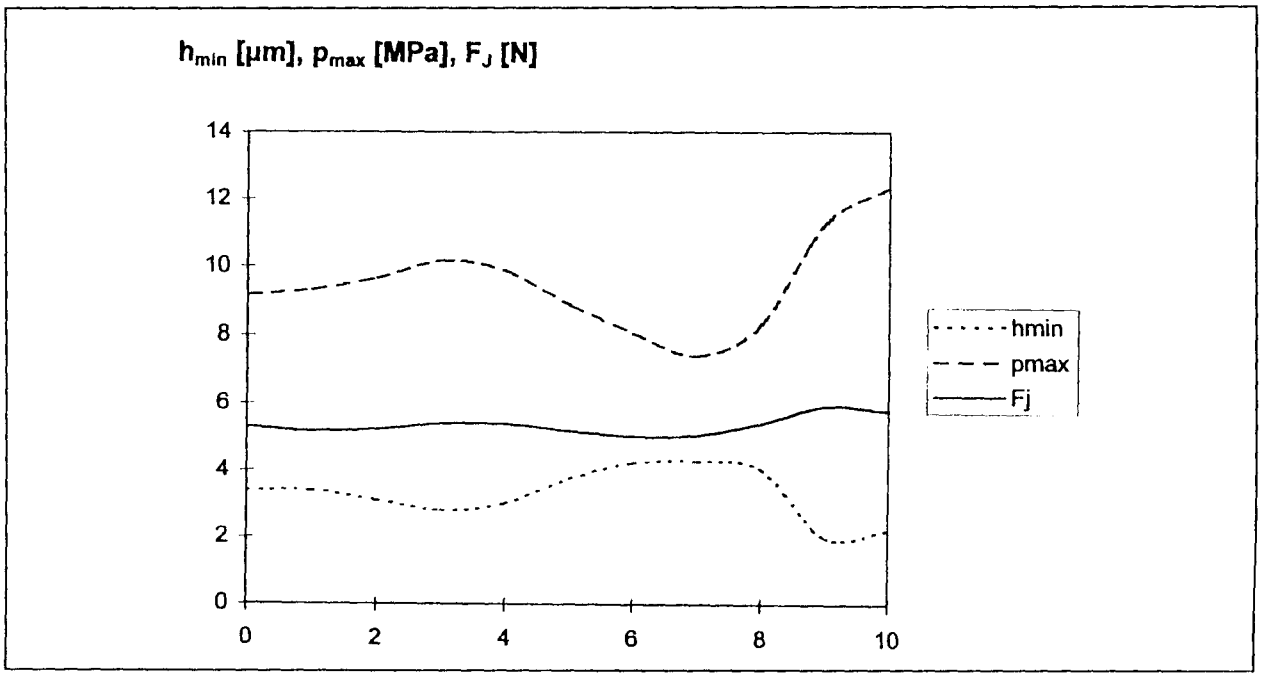

Fig. 4 Calculated results for a combined Multi-Wave bearing N_l=5.50, W_c=2.50 m, W_l=2.50 μm, n=0.00742 Pa.s, N= 3000 rpm Reference calculation configuration

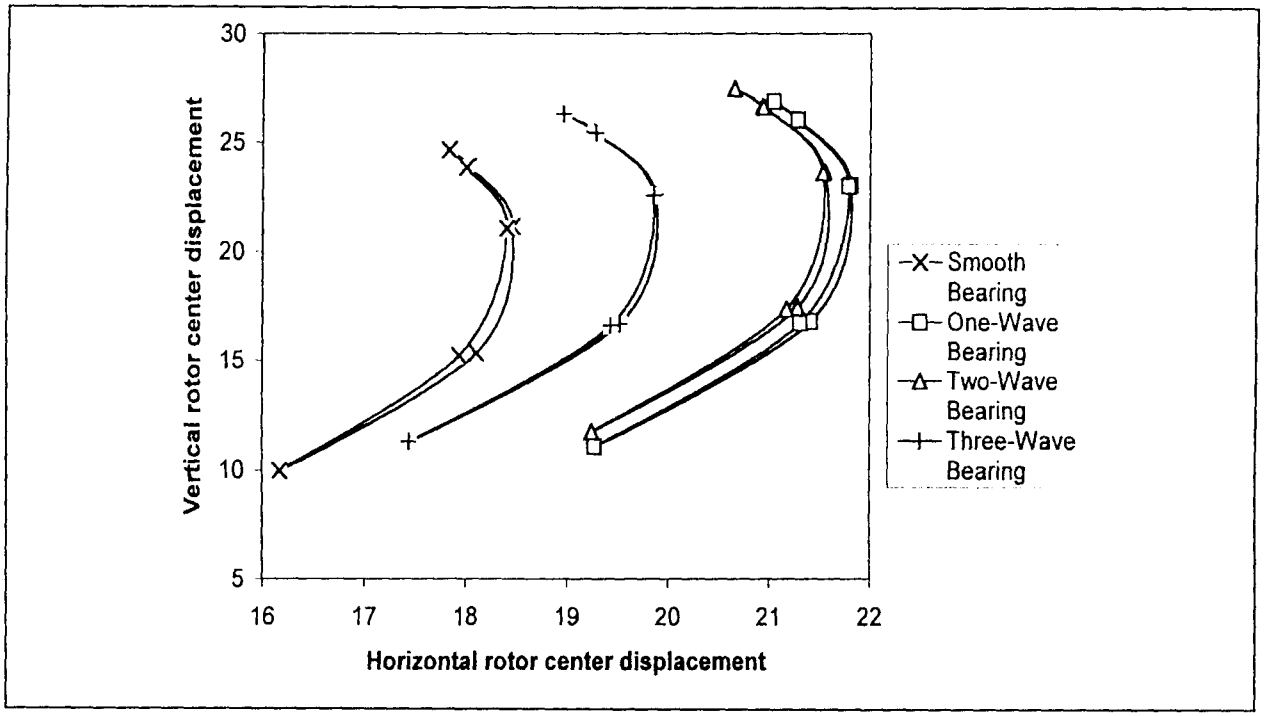

Fig. 5 Journal center path under dynamic loading related to bearing center for a combined wavy bearing N_l=5.50, W_c=2.50 m, W_l=2.50 μm, n=0.00742 Pa.s, N= 3000 rpm Reference calculation configuration

During the sinusoidal loading conditions the squeeze contribution in load support creates small hysteresis concerning the journal center position magnitudes curves (Fig. 5). On the other hand, in the case of the friction forces curves hysteresis is insignificant.

The actual number of waves (N_c and N_l) must be selected on the basis of the actual rotor-rotating load. The wavy bearing configuration characterized by waviness number and its amplitude can be optimized for each specific application. Any optimization concerning the journal-bearing geometry cannot be realistic without the development of a mixed model taking into account journal-bearing asperity contacts [7-9].

REFERENCES

[1] *Arnold O., Schultheiss H. and Glaser H .*, "**Experimental investigation into the oil flow rate and the friction moment of dynamically loaded plain journal bearings**", Proceedings INTERTRIBO '99, Slovak Republic, 1999, pp. 285-288.

[2] *Cameron A.*, "**Basic Lubrication theory**", Ellis Horwood Ltd, 1981.

[3] *Christensen H.*, "**Stochastic Models for Hydrodynamic Lubrication of Rough Surfaces**", Proc. Inst. Mech. Eng. Tribology Group 184, Part 1, Vol. 55, 1970, p. 1013.

[4] *Christensen H.*, "**A Theory of Mixed Lubrication**", Proc. Inst. Mech. Eng., Vol. 186, 1972, p. 421.

[5] *Dagnall M.A.*, "**Exploring surface texture**", Rank Taylor Hobson Ltd, Leicester, 2nd edition, 1986.

[6] *Dimofte F.*, " **Bearings with non-conventional geometry (or wave bearings)-an advanced bearing technology**", Proc. 3rd Int. Conf. BALKANTRIB '99, 1999, pp. 425-440.

[7] *Greenwood J.A.*, "**The area of contact between rough surfaces and flats**", Journal of Lubrication Technology, Jan. 1967, pp. 81-91. [8] Greenwood J.A. and Tripp J.H., "The contact of two nominally flat rough surfaces", Proc. Inst. of Mech. Eng., Vol. 185, 1971, pp. 625-633.

[9] *Handzel-Powierza Z., Klimczak T. and Polijaniuk A .*, "**On the experimental verification of the Grennwood-Williamson model for the contact of rough surfaces**", Wear 154, 1992, pp. 115-124.

[10] *Kruszynski B. and van Luttervelt K.A .*, "**The influence of manufacturing processes on surface properties**", Adv.Manuf.Engg 1, 1989, pp. 187-202.

[11] *Lin J.R.*, "**Steady state performance of finite hydrodynamic journal bearing with three-dimentional irregularities**", ASME, J. Tribol. 112, 1990, pp. 497-505.

[12] *Lin J.R.*, "**Squeeze film characteristics of finite journal bearings: couple stress fluid model**", Tribology Intern. Vol. 31, Nr 4, 1998, pp. 201-207.

[13] *Noizat J.*, "**Viscosite limite admissible des lubrifiants faible viscosite dans les paliers**", E.C.L-DLA/DRDA/RNUR, Paris-France, 1985.

[14] *Pandazaras C.N.*, "**Etudes Experimentales et Theoriques sur les Pertes par Frottement dans les Ensembles Pistons-Segments-Chemises**", Etude Bibliographique, DLA/DRDA/RNUR - ISMCM, Paris-France, 1982.

[15] *Pandazaras C.N.*, "**Modelisation du Frottement Segment-Chemise**", DLA/DRDA/RNUR, Note Thechnique No 5781, Paris-France, 1982.

[16] *Pandazaras C.N.*, "**Influence de la Forme des Segments sur le Frottement Segment-Chemise**", DLA/DRDA/RNUR , Note Thechnique No 5808, Paris-France, 1983.

[17] *Pandazaras C.N.*, "**Modelisation Theorique et Experimentale du Frottement Segment-Chemise**", These D.D.I., ISMCM - DLA/DRDA/RNUR, Paris-France, 1985.

[18] *Pandazaras C.N.*, "**RENAULT Ring-Liner Friction Code**", JRC-PG Tribology in Power Train, (PSA-FIAT-VOLVO-B.L.-RENAULT) DLA/DRDA/RNUR, Paris-France, 1985.

[19] *Pandazaras C., Petropoulos G and Koutlas G.* "**Numerical Modelling of the Functional Behaviour of Finite Sliding Hydrodynamically Lubricated Journal Bearings Considering Surface Macrogeometrical Deviations and Dynamic Loading**", Journal of the Balkan Tribological Association, Vol.5, No 3, 1999, pp.202-210.

[20] *Patir N. and Cheng H.S.*, "**An average model for determining effects of three dimensional roughness on partial hydrodynamic lubrication**", Trans. ASME, vol. 100, 1978, pp.12-17.

[21] *Patir N. and Cheng H.S.*, "**Application of average flow model to lubrication between rough sliding surfaces**", Trans. ASME, vol 101, 1979, pp.220-230.

[22] *Peters J. and al*, "**Assessment of surface typology analysis techniques**", Annals of the CIRP, 28/2, 1979, pp. 539-553.

[23] *Petropoulos P.*, "**A note on the homogeneity of the roughness on oblique finish turned surfaces**", Wear, 24, 1973, pp.147-152.

[24] *Petropoulos G., Pandazaras C. and Stamos I.* , "**Developing predictive models between selected texture parameters of turned surfaces**", Journal of Balkan Tribological Association, Vol.5, No 3, 1999, pp. 156-170.

[25] *Pranab K.Das*, "**Analysis of Piston Ring Lubrication**", SAE Paper 760008, 1976, pp. 1-10.

[26] *Rank Taylor Hobson*, **Handbook**, Version 1.1.1, 1995.

[27] *Rasheed H.E.*, "**Effect of surface waviness on the hydrodynamic Lubrication of plain cylindrical sliding element bearing**", WEAR 223, 1998, pp. 1-6.

[28] *Rohde S.M.*, "**A mixed friction model for dynamically loaded contacts with application to piston ring lubrication**", General Motors Research Laboratories, 1980.

[29] *Strzelecki S. and Someya T .*, " **Static characteristics of the off-set halves journal bearing**", Proceedings INTERTRIBO '99, Slovak Republic, 1999, pp. 289-292.

[30] *Strzelecki S.*, "**Journal centre trajectory of dynamically loaded offset-halves bearing**", Proceedings BALKANTRIB '99, Sinaia-Romania 1999, pp. 373-378.

[31] *Strzelecki S.*, "**Friction Loss of 2-lobe journal bearing with different bush profile**", Proceedings BALKANTRIB '99, Sinaia-Romania 199**9, pp. 379-386.**

[32] ***Teale J.L. and Lebeck A.O.,*** "**An evaluation of the average flow model for surface roughness effects in lubrication**", Trans. ASME, vol 102, 1980, pp.360-367.

[33] *Tripp, J.H.*, "**Surface roughness effects in hydrodynamic lubrication: the flow factor method**", Transactions of the ASME, Vol. 105, 1983, pp. 458-465.

[34] *Tzeng, S.T. and Saibel, E.*, "**Surface roughness effects on slider bearing lubrication**" ASLE, Vol. 10, 1967, p.334.

[35] *Whitehouse D.J.*, "**Handbook of surface metrology**", Institute of Physics publishing for Rank Taylor Hobson Co, Bristol, 1996.

UDK 621.192.6.004

D. JOSIFOVIĆ, S. MARKOVIĆ

Damages and Methods for Regeneration of The IC Engine Piston Mechanism Elements

RESEARCH

1. INTRODUCTION

Tough exploitation conditions in which operate the piston mechanism elements of an IC engine (elevated temperatures, high loads, necessity for maintaining the high degree of hermeticity of the combustion chamber, high nonuniformity of speeds of motion), assume high requirements for their production and regeneration. The mentioned working conditions enable significant wear of the piston mechanism elements, as well as their mechanical and thermal damages. Operation of the engine with the worn piston mechanism elements leads to decrease of the engine power, increase of the oil and fuel consumption, appearance of smoke and soot, impacts, increased noise, and other irregularities.

2. DAMAGES OF THE PISTON MECHANISM ELEMENTS

The most frequent piston damages (Figure 1) are:

A - deposition of soot, scale and resin,

B - front burns,

C - wear of the piston outer surface,

D - wear of channels for piston rings along the height and depth,

E - wear of the hole for the piston axle.

Piston rings are removed from exploitation due to burns and wear of the outer surface and rings height.

Ph. D. D. Josifović, Professor,
MS Svetislav. Marković, Lecturer,
Faculty of Mechanical Engineering, Kragujevac

On piston axles, wear appears on the outer surface, as well as small cracks.

The following damages can be noticed on piston rods (Figure 2):

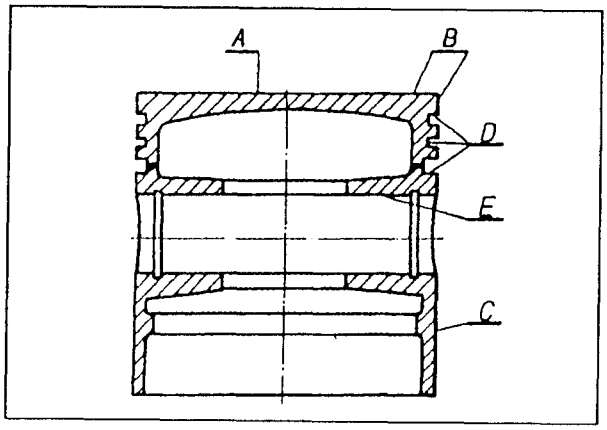

Figure 1. Damages of the IC engine pistons

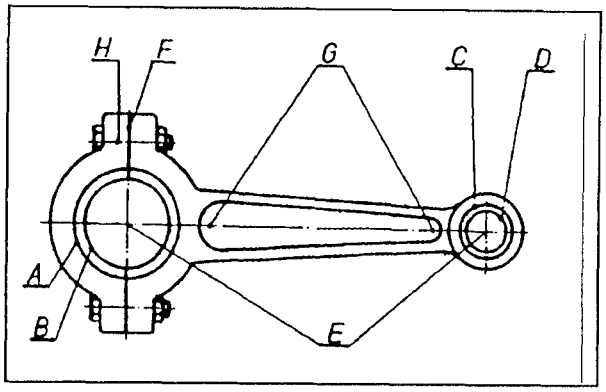

Figure 2. Damages of the IC engine piston rods

A - wear of the piston rod large crosshead hole,

B - wear of the piston rod large crosshead bearing, and dame of the exhaust for fixing the bearing liners,

C - wear of the piston rod small crosshead hole,

D - wear of the bearing (sliding bush) of the small crosshead,

E - non-parallel positions of the piston rod large and small crossheads holes - bending and torsion of the piston rod,

F - damage of the bearing surfaces for separation of the piston rod and the large crosshead cap,

G - cracks on the piston rod,

H - wear, shearing of threads and fracture of screws for connection of the cap with the piston rod, as well as of the threads of the large crosshead cap.

The most frequent damages of the crankshafts (Figure 3) are:

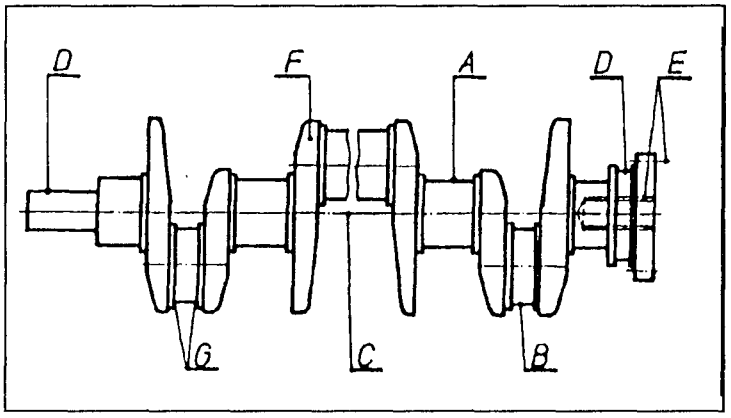

Figure 3. Damages of the IC engine crank shafts

A - wear of the supporting (bearing) necks,

B - wear of the flying necks,

C - shaft flexure,

D - wear of necks to which the seals and distributing gear are fitted,

E - wear and damages of grooves, threaded and other holes,

F - appearance of cracks on the shaft,

G - plastic deformation of the cranked portions, namely different distances between the single cranked portion walls.

Consequence of uneven wear of necks if appearance of conicity and ovality.

3. DIAGNOSTICS

In diagnostics of the piston mechanism elements several methods can be applied:

Visual method detects the burns of the piston front and piston rings, damages of threads, larger cracks, changes of shapes and fractures of the piston mechanism elements, as well as the jams, and scratches on the piston axle and crank shaft cranks.

The technical measurements method is used for determination of the magnitude of wear, deformation, flexure and warping of the piston mechanism elements. Defectoscopic methods, primarily magnetic as well as radioscopic, ultrasonic and penetrating ones, are applied for detection of the hidden cracks on piston rods, piston axles, and the crankshaft.

The technical measurements method enables determination of wear magnitude of bearings and holes, check of their conicity and ovality, detection of flexure and warping of piston rods (non-parallel positions of small and large crosshead holes axes) and similar damages. When an IC engine is completed the piston rods masses are measured, assembled with bearings, screws, and nuts. Piston rods that are built into an engine must have approximately equal masses. Unequal masses of piston rods disturb the quiet operation of the crankshaft and cause undesired vibrations. For detection of small cracks, the magnetic method is applied. Measuring of the piston rod warping is done with the bearing (bush) of the small crosshead, but without the large crosshead bearing. The procedure is as follows (Figure 4, a): in the large crosshead is placed the axle, which is, by its ends supported in prisms (3), placed on the measurement plate (2). With help of the comparator the position of this axle is determined (I-I), at a distance L (usually *200 mm*). With the adjusting screw (4) the piston rod (1) is brought into the approximately horizontal position. Then, again with the use of comparator, the difference in height between the axle's ends is determined, after it is fitted into the small crosshead bearing (II-II), at distance L. The difference in height between the axle's end points (position

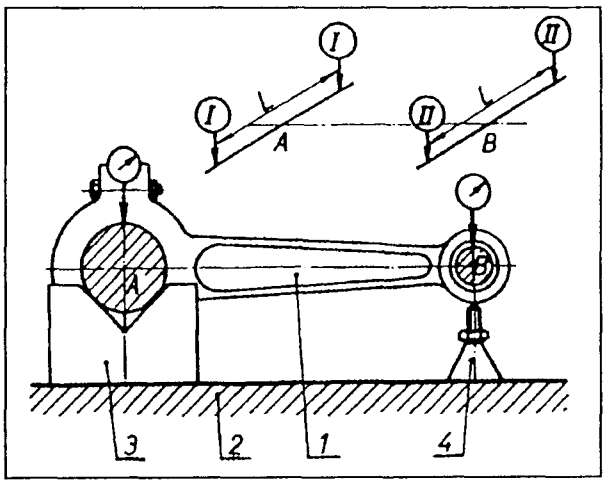

Figure 4. Piston rod checking, a) of warping; b) of flexure

II-II), corrected by eventual difference in height between the large axle's end points (position I-I), represents the piston rod warping, i.e., the non-parallel position of small and large crossheads holes axes, in horizontal plane.

The procedure of piston rod flexure is similar to the previous one (Figure 4, b). The only difference is that the piston rod (1) is, with help of the adjusting screw (4), brought into approximately vertical position. The difference in height between the axle's end points (position III-III), corrected by eventual difference in height between the large axle's end points (position I-I), represents the magnitude of the piston rod flexure, i.e., the non-parallel position of small and large crossheads holes axes, in vertical plane. The difference in height between the large axle's ends (position I-I) in both cases is the constant value, that depends exclusively on accuracy of the manufacturing of prisms.

It is also frequently necessary to check the paralellity of positions of the large crosshead hole and the separation surface between the piston rod and the large crosshead cap.

Necessity of crack shaft regeneration, and substitution of bearings, is determined according to ovality of necks, and exceeding of permissible clearances in bearings. Clearances are determined for each type of engines, and for each crankshaft regeneration measure, according to corresponding technical conditions. In crankshafts diagnostics, special attention should be devoted to working surfaces of bearing and flying necks and bearings, clearances in bearings, distances between the cranked portion walls, and radial eccentricity of flying necks.

Bearing and flying necks of the crank shaft are, for example, measured in two mutually perpendicular planes, vertical and horizontal, and at three points along the length (Figure 5). Vertical measuring plane of necks assumes the surface that passes through the bearing and flying necks axes. The horizontal measuring plane corresponds to the surface perpendicular to the vertical one. The two end measuring areas are at a distance *0.4 l* from the neck middle. The conicity, ovality and oil clearance

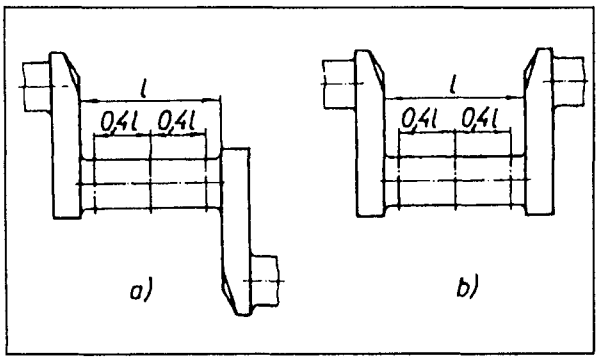

Figure 5. Measuring points for a) bearing and b) flying necks.

magnitude are determined according to performed measurements.

Clearances in bearings are measured by the measuring heads, or lead imprints. Permissible value of the oil clearance is usually larger than the normal clearance in sliding bearings, and for each following repair measure it is decreased for *0.02-0.03 mm*, with respect to the previous one.

The shaft deflection is determined by use of the comparator, at three sections of the shaft, at its end and in the middle. If the crankshaft eccentricity does not exceed *0.1 mm* for automobile engines, and *0.2 mm* for the heavy engines, they are not subjected to straightening. Damage is removed by grinding. Checking of the shaft flexure can be done also for the frontal eccentricity of the flange for fixing the flywheel. Maximum allowed eccentricity is *0.05 mm*.

Eccentricity of the flying necks of the crankshaft, placed on the flying necks, is determined by the comparator of the clock type that is fixed for the holder. The value of eccentricity is determined as a difference between the smallest and the highest reading-off from the comparator's arrow, for the full rotation of the shaft, at two section at a distance of *0.4l* from the middle point of the neck, to both sides. The distance between the crank portion walls is measured by the special equipment with the clock type indicator. The device is placed between the walls of the cranked portion, the arrow is brought into the zero position, and then the shaft is rotating slowly.

4. REGENERATION METHODS FOR PISTON MECHANISM ELEMENTS

The piston regeneration is reduced to reaming of the hole for the piston axle by the manual reamer. The hole diameter must correspond to the piston axle. Besides that, if the damage remained within the allowed limits, the channels must be cleaned, and the sooth, scale and resin must be removed.

The piston axle is regenerated by grinding to the repair size, and by polishing or hard chromizing, and then grinding.

Worn and damaged inside surfaces of the small and large crossheads, as well as damaged separation surface of the piston rod and the large crosshead cap, can be regenerated by hard facing and subsequent mechanical machining of surfaces to the nominal sizes. The repair measures application is also possible [2].

Small cracks that do not pass through the whole cross section can be regenerated by hard facing.

Due to plastic deformations, or due to performed regeneration work, the impermissible decrease of the be-

tween-axes distance of the piston rod holes can occur. Shortening of the piston rod leads to increase of the combustion chamber, decrease of compression and engine power. In order to extend the piston rod, it is necessary to place the large crosshead cap, and fasten the screws, so that on the separation surfaces remains the clearance of *1.5-2 mm*. Then the piston rod (4) is placed on the special device (Figure 6), that consists of the steel plate (1) to which are fixed two axles (2 and 6), whose diameters correspond to holes' diameters. The distance between their axes must be identical to nominal distance between the axes of the piston rod holes. After the piston rod, the steel plate (3) is placed on the axles, and fastened by screws. Then, the middle part of the piston rod, of length *60-70 mm*, is heated by the high frequency current, by use of an inductor (5), or the gas burner, up to the temperature of *300-400°C*, in order to remove the inside stresses. Such a regeneration procedure is allowed to perform be only once per one piston rod.

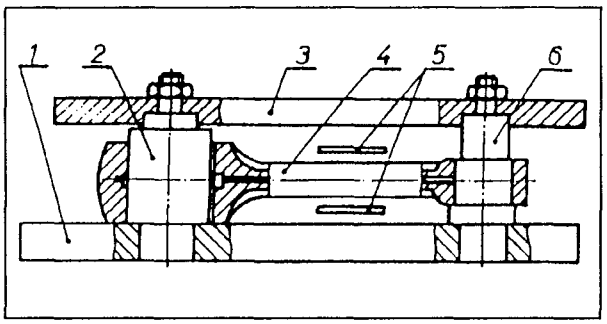

Figure 6. Device for the piston rod stretching

The basic operation of the crankshaft regeneration represents grinding of the bearing (Figure 7) and flying necks (Figure 8), to the repair sizes.

The crank shaft necks grinding is done on special grinding machines, with necessary application of devices that enable correct placing and control of that placing of the shaft, prior to grinding.

The flying necks are ground during placing the crankshaft in fixtures eccentrically, where it is fixed by its end bearing necks. Eccentricity enables moving of the shaft for a crank radius, and bringing the flying necks axes to coincide with the grinding machine spindle (Figure 8).

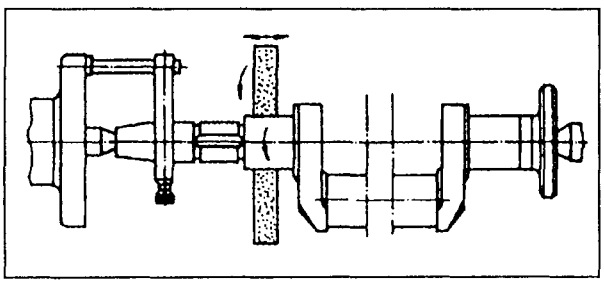

Figure 7. Grinding of the basic (bearing) necks

The flying necks axes must be parallel to the bearing necks axes. The flying and bearing necks must be ground to the same repair size, with differences in diameters less than *0.05 mm*. During grinding the special attention should be paid to transition from the neck working surface to the cranked portion wall. This transition must be smooth, so the inside stresses would be removed, and the crankshaft fracture prevented.

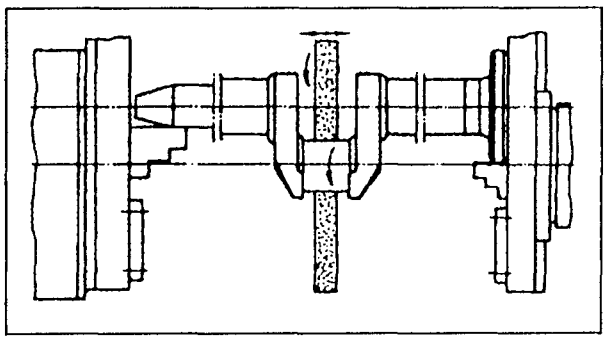

Figure 8. Grinding of the flying necks

All the necks of the crankshaft must be subjected to polishing or super-finishing. Polishing causes the plastic deformation - ironing of the surface roughness, while the super-finishing increases the wear resistance.

The crank shaft necks, that are worn so much that they can not be regenerated by any of the repair measures, can be regenerated to the nominal sizes by the vibro-arc welding, automatic hard facing under the melting layer, and by the powder electrodes without thermal treatment, by electrolytic polishing and metallization. After these regeneration methods, the straightening of the crankshaft necks is performed, then grinding and polishing or super-finishing of the regenerated necks.

On the regenerated basic and flying necks, the quality of machining is controlled, as well as conicity and ovality.

Regeneration of the worn necks for placing the seals, rolling bearings, distributing gear and belt pulley for the fan drive, is done by electrolytic deposition, or vibro-arc facing, with subsequent mechanical machining to nominal sizes. The choice of methods depends on the extent of wear, [1].

The worn walls of the cranked portions of the flying necks are regenerated by machining to a larger size. The bent crankshafts are straightened in the cold state, on a hydraulic press (Figure 9). After straightening, the shaft is controlled for eccentricity of the middle neck. The deformed cranked portion walls are straightened by forging with the pneumatic hammers or manually. Depending on the direction of the crank shaft flexure, the corresponding surfaces of its flying neck left hand side or the right hand side walls are forged, with such force that as a result of the ensuing compressive stresses and walls' deforma-

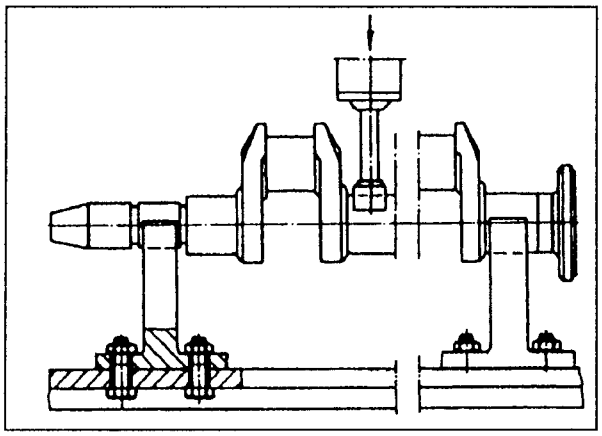

Figure 9. The crank shaft straightening

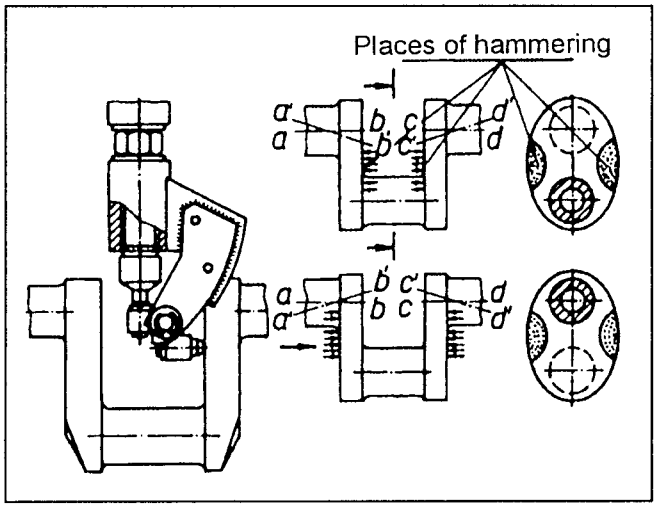

Figure 10. Scheme of the crank shaft straightening by forging of the flying neck walls with a pneumatic hammer (a'b' and c'd' - positions of necks axes before straightening, ab and cd - positions of necks axes after straightening).

tions the necessary displacement of the necks' axes is obtained, Figure 10.

Regeneration of the screw holes on the crankshaft flange for fixing of the flywheel is done together with the flywheel, to the increased repair sizes.

The crankshaft after regeneration must be subjected to dynamic balancing. Imbalance of the shaft is removed by drilling of holes in necks or by counter weights placed on the shaft. The allowed magnitude of imbalance for the agricultural machines' crank shafts is *120 gcm*, for trucks shafts is *100-150 gcm*, and for light vehicles *10-50 gcm.*

Bearing and flying bearings of contemporary engines represent mutually changeable steel or bronze inserts, soldered by the anti-frictional layer of thickness *0.2-1 mm*. Worn inserts of bearing and flying bearings of all the engines, as a rule, are replaced by new ones, with smaller repair sizes, according to measures of crank shaft necks after their grinding, or they can be regenerated by deposition of polymer materials.

During the piston mechanism elements regeneration the control of lubricating channels is mandatory, both on crankshaft and on piston rods, and their rinsing on special devices.

5. ECONOMIC EFFECTIVENESS OF REGENERATION

Economic effectiveness of the IC engine piston mechanism elements regeneration is extremely high: the regeneration price ranges between *5* and *40%* of the price of the new elements. There the similar working life of the regenerated element is achieved. Thus, regeneration of the crankshaft to repair sizes makes *5-10%* of the new shaft price (for larger engines it is below *5%*), and the working life is over 90 % of that of the new shaft.

6. CONCLUSION

The diversity of technically reliable and economically justified regeneration methods of the IC engine piston mechanism elements is obvious. It can be stated, with certainty, that the IC engine parts are the machine elements that are most frequently being regenerated in our repair practice.

REFERENCES

[1.] *Marković S., Josifović D .*: **Techno-economic justification of the railway engine crank shaft regeneration** , "Tribology in Industry", XIX/3, September 1997.

[2.] *Marković S., Josifović D.* : **Constructive changes on the connecting rods of the railway engine based on results of the repair diagnostics** , Proceedings of the 10. International Symposium "Motor vehicles and Engines MVM'98", Kragujevac, October 5-7, 1998., pp. 369-372.

[3.] *Petrov J. N., et al .*: **Fundamentals of the machine repair**, "Kolos", Moscow, 1972.

[4.] *Schwoch W.*: **Das Fachbuch Vom Automobil Automotor**, Georg Westermann Verlag, Braunschweig, 1976.

[5.] *Uljman I. E., et a* l.:**Remont mašin**, "Kolos", Moscow, 1967.

UDK 621.533.38.001.5

RESEARCH

R. RAKIĆ

The Influence of Lubricant on The Reliability of Open Gears

The aim of this study is to investigate the influence of lubricating greases on the reliability of open gears. The experimental investigations of the tribological aspects of lubricating grease choice for open gears and the effects of lubricating greases properties on tribological behavior of open gears have been carried out on machine tools. The paper presented the following:

- *The analysis of the kinds of lubricating greases for open gears,*
- *The flowchart for the selection of the lubricating grease for open gears in function of all relevant influential factors,*
- *The analysis of the symptoms of failure to open gears,*
- *The analysis of the failure rates and the average life of open gears,*
- *The curves of open gear reliability in function of tribological properties of lubricating greases under presented operating conditions of investigation.*

The reliability of open gears was found to be affected by both NLGI consistency number and type of lubricating grease under presented operating conditions.

Keywords: *open gears, lubricant, reliability*

1. INTRODUCTION

Gears are vital power transmission elements in machines. Many studies have been carried out all over the world to understand the functional behavior of gears during service. The main emphasis has been on the contact, fatigue failure, durability, etc. A good understanding of tribological processes and various types of gear failures, is necessary for selection of gear material, lubricant, reliability and life estimation of gears. Under normal running conditions, the gears operate under elastohydrodynamic conditions where there is a highly pressurized film of lubricant holding the mating teeth apart [1]. Future scientific and technological task is development of materials for highly stressed tribological components, including gears, bearings, seals and actuators with reduced or even zero maintenance [2].

For gears, numerous methods have been developed to calculate the thickness of these films, including those by Dowson and Higginson [3], Hamrock [4] and the others. The differences in the formulae apply primarly to different contact geometry.

It is well known that concentrated contacts, such as those found in gears and rolling bearings, are lubricated by a thin film formed elastohydrodynamically at the edge of the Hertzian contact [5]. There is now an extensive body of literature in elastohydrodynamic lubrication (EHL) to describe the behavior of film thickness, pressure, sliding friction and contact temperature [6] and the others.

Dr. Ing. Radoslav Rakić,
NIS-Naftagas promet, Novi Sad, Yugoslavia

2. OPEN GEARS

Open gear drives are not enclosed in a sealed gearcase. They are commonly subjected to harsh environmental conditions. Physical size, loading cycles, metalworking particles can cause tribological processes (misalignment, vibration, and so on) which can manifest as rapid, irregular wear on gear teeth and failures. On this type gear often the lubricant is applied only from time to time. Only a thin film exists between the teeth as shown in Figure 1.

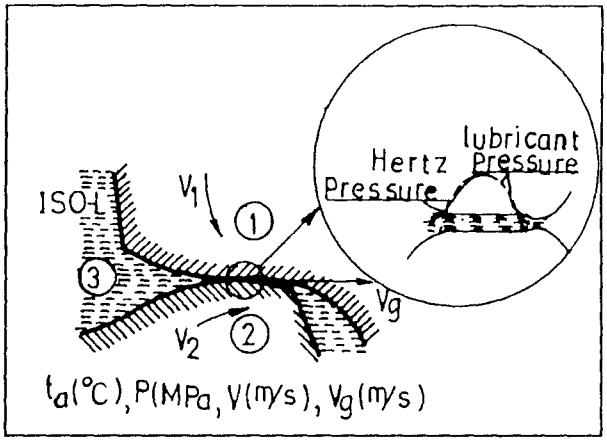

Figure 1. Schematic illustration of gears

There is another important factor which must be considered. The revolving gear tends to throw the lubricant of the gear teeth by centrifugal force. Therefore, the lubricant also has to have an adhesiveness, a tackiness, that makes it stick to the teeth under these conditions.

This tribomechanical system, as shown in Figure 1, consists of three elements, these being : the element 1 (gear 1), the element 2 (gear 2) and the element 3 (lubricant) in which the contact between the two former elements is realized. The gears have poor conformity between surfaces, very small contact areas and very high unit loading.

The tribological behaviour of the open gear is influenced by a number of factors that are interrelated in complicated ways. The main influential factors are: t_a - ambient temperature, p-Hertz pressure, V_g - sliding velocity and V - pitch velocity.

3. LUBRICANT

On open gears, even more than flooded gears, you need a lubricant of such film strength and adhesiveness, such lubricating value, that it will not be squeezed out at the point of mesh. With modernization of the industry, lubrication requirements for open gears have undergone considerable change. Lubrication requirements of these gears depend on the type of application, type of gear, ambient temperatures and the teeth operating conditions.

Table 1. Classification of lubricants for open gears

A	B	C
Products usually of bituminous type with anti-corrosion properties	CKH	Cylindrical or bevel gears operating at medium ambient temperatures and generally under light load
Products of CKH type with enhanced extreme-pressure and anti-wear properties	CKJ	
Greases with improved extreme pressure, anti-wear and anti-corrosion properties and improved thermal stability	CKL	Cylindrical or bevel gears operating at high or very high ambient temperatures and under high load
Pasty products with improved anti seizing properties that permit use under extreme loaded conditions and anti-corrosion properties	CKM	Gears operating occasionally under exceptionally high loads

Open gears lubricants generally fall into three categories, viz. lubricants of bitumenous type, soap based greases and pasty products. The classification of lubricants for open gears are shown in Table 1 [7] where are: **A**-Composition and properties, **B**-Symbol ISO-L, **C**-Typical application. However, the trend worldwide is towards replacement of bituminous compounds with soap based greases. Lithium and aluminium based greases are generally the preferred base for formulation of open gear lubricant. Additionally tackiness improvers, EP/anti-wear additives and solid lubricants are also used in the formulations.

4. SELECTION PROCEDURE OF LUBRICATING GREASE

A lubricating grease may be defined as a solid or semi solid dispersion of a thickener in a liquid lubricant, fortified with various additives depending upon its intended application. The kinds of lubricating greases with standpoint recommendations for the choice of lubricants for machine tools are given in [8] and ISO Classification, Family X(greases) are given in [9].

To achieve optimum possibility for investigation of the effects of tribological properties of lubricating greases on the open gears failures of machine tools, the author has presented the flowchart for determining of the NLGI characteristic of lubricating greases in Figure 2. For this selection procedure, four essential parameters have been taken into account. These are:

- Lower operating temperature (the second (2.) letter),
- Upper operating temperature (the third (3.) letter),
- Water contamination (the fourth (4.) letter),
- Load (the fifth (5.) letter).

5. EXPERIMENTAL INVESTIGATION

Table 2. Working conditions of open gears and other influential factors

Operating conditions:	
Type of motion	rolling/sliding
Frequency of motion	irregular
Sliding velocity	low ($V_g \leq 1$m/s) $V_g \leq 1/3$ V
Contact stress	low ($P \leq 500$ MPa)
Contact geometry	line
Environment:	
Lower operating temperature	$t_l \geq -15°C$
Upper operating temperature	$t_u \leq 70°C$
Medium	Static moisture and contaminants
Open gears (element 1and 2)	
Composition	steel
Hardness	high (>500HV)
Surface condition	smooth
Coating	no coating
Lubricant (element 3):	
Condition	lubricated
Type	lubricating greases: ISO-L-XCCDA ISO-L-XCCEB ISO-L-XCFHB
Consistency	NLGI 2 NLGI 3

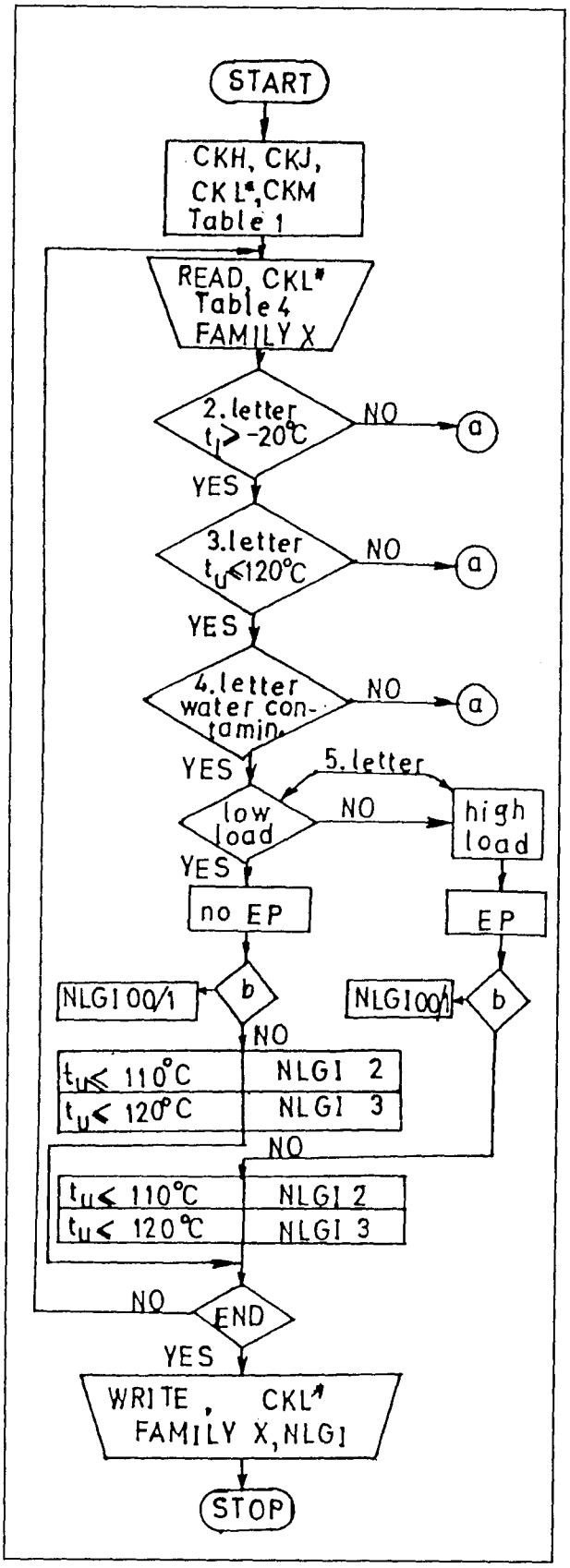

Figure 2. Flowchart of grease selection procedure, a- Go to the other model of decision making, b- centralized system.

The experimental investigations of the influence of lubricating greases on the reliability of open gears have been carried out on machine tools. Figure 3 illustrates experimental machine tool with open gears (rack)/toothed segment in the machine assembly. Working conditions of these open gears are shown in Table 2.

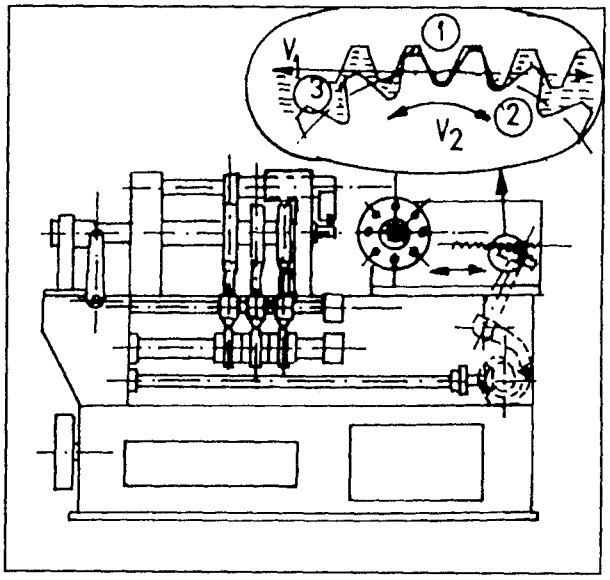

Figure 3. Machine tool with identified open gears

The relevant parameters of the test procedure on the experimental machine tool (Fig. 3) are shown in Table 3.

The experimental investigation of the influence of lubricating greases on open gears failures are presented for two NLGI consistency numbers and three types of lubricating greases.

Table 3. The relevant parameters of test procedure for open gears

Main symptoms of failure	Relevant parameters
1. Excessive clearance	h-backlash h_{max} =0,15 - 0,40 mm
2.Decrease of machining accuracy	τ - tolerance of cutting operation
3. Untrue running	Wobbling of gear
4. Corrosion	Corrosion due to moisture and contaminants
5. Breakage of teeth	Fatigue crack (pitting)
6. Other symptoms	Contamination

The problems appearing at all gears very often represent the consequences of tribological processes development on their contact surfaces. The tribological processes on contact surfaces of gears have been studied by author [10, 11, 12, 13] in fiunction of all influential factors.

6. RESULTS OF EXPERIMENTAL INVESTIGATION AND DISCUSSION

Author discussed three major measures of gears reliability effectiveness:

- Failure rate -λ,
- Average life - $\overline{T}_c$
- Reliability curve $R(T)$

The life time of the gears up to the failure mostly shows large deviation. By the aid of probability and statistic methods, it was possible to determine the influence of lubricating oils on the reliability of open gears. This procedure consists of evaluating the appropriateness of the fit by using a specific test like χ^2 test. The most familiar way to test for Poisson/exponential character is to use χ^2 goodness - of - fit test on the data presented in Figure 4, 5 and 6 from against a theoretical distribution, with the parameter replaced by its maximum - likelihood estimator. The resulting stastistic is then:

$$\chi_i^2 = \sum_{i=1}^{n} \frac{(f_i - f_{t_i})^2}{f_{t_i}}$$

where f_i is the number observed in the i-th frequency class, f_{it}, is the number expected in the i-th frequency class if the hypothesized distribution were correct, and k is the number of degrees of freedom, always equal to the total number of classes less one and then minus one for each parameter estimated. The results for three periods of time were plotted in the reliability curves versus time shown in Figures: 4, 5 and 6. These curves represent the probability of the open gears reaching the moment >>T.

According to Figures: 4, 5 and 6 it can be seen that curves R(T) for open gears in presented operating conditions of investigation have approximately exponential distribution. The variation of the reliability with time follows

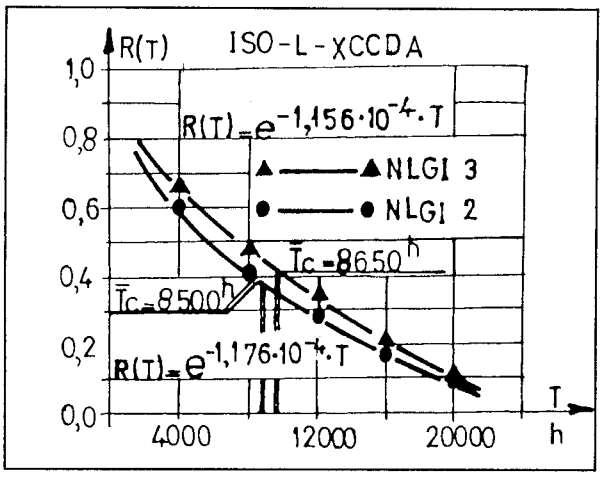

Figure 4. Reliability of open gears for lithium grease ISO-L-XCCDA

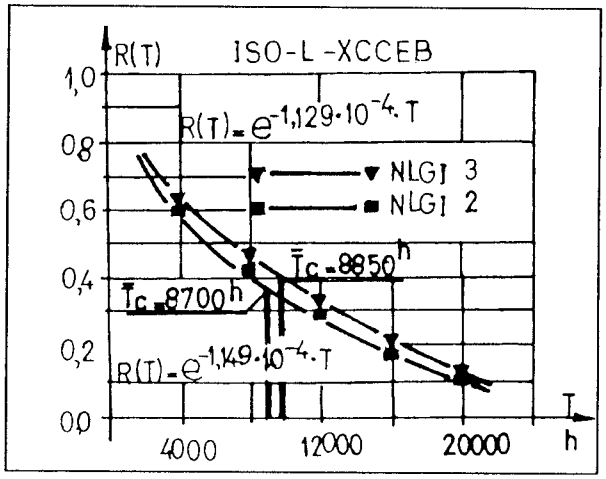

Figure 5. Reliability of open gears forlithium grease ISO-L-XCCEB

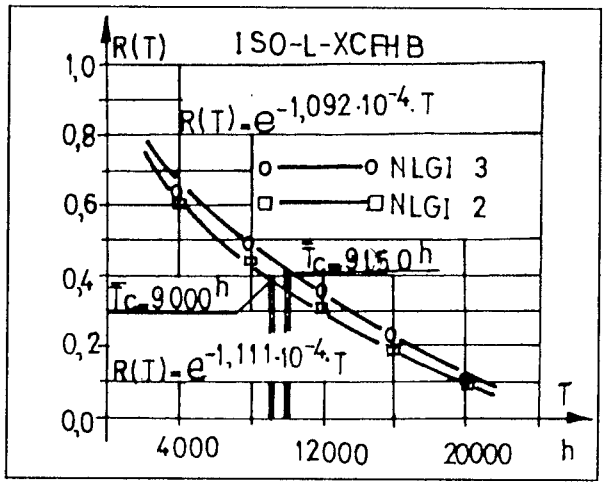

Figure 6. Reliability of open gears for aluminium grease ISO-L-XCFHB

an exponential law. This procedure consists in evaluating the appropriateness of the fit by using a specific χ^2 test like the test. For example, χ^2 test for data of figure 4 is shown in Table 4. Based on χ^2 test for these data ($\chi^2 < \chi_{0.05}^2$), it can be concluded that reliability curves are approximately exponentially distributed.

According to working conditions of open gears on machine tool and grease properties, the consequent differences in life in relation to grease properties are:

- *The effect of grease type and thickener type*
  The aluminium-base grease compared with lithium-based greases obviously gave the longest lives among these tested greases. The aluminium - based grease, because of high water-resistance, exellent corrosion resistance and high drop point (for operating temperatute up to $+1800°C$) make it very well suited for lubrication of open gears operated under irregular load and high moisture presence due to coolant system for metalworking. This grease provides effective protection against wear due to aluminium complex soap system.

- *The effect of EP additive*
  According to Figure 4, 5 and 6 it can be concluded that the improvement of open gears lives by the EP additive was significant. The aluminium grease with EP additive and lithium grease with EP additive have a longer open gear life compared with the case of lithium grease without EP additive.
- *The effect of consistency number*
  As expected the increase of consistency number improved the open gear life. However, the effect of consistency number to lives was less compared with that of changing grease type.

In Table 4 are: $A = T(h)$, $B = f_i$, $C = f_{it}$,
$D = (f_i - f_{it})$, $E = (f_i - f_{it})^2$, $F = (f_i - f_{it})^2 / (f_i - f_{it})$

Table 4. χ^2 test for data of Figure 4

A	B	C	D	E	F
0-3000	16	17.76	-1.76	3.10	0.1745
3001-6000	14	12.66	1.34	1.80	0.1422
6001-9000	9	8.80	0.20	0.04	0.0045
9001-12000	5	6.13	-1.13	1.28	0.2088
12001-15000	4	4.39	0.39	0.15	0.0341
15001-18000	3	2.99	0.01	0.00	0.0000
18001-21000	3	2.23	0.77	0.59	0.2646
21000	6	5.04	0.96	0.92	0.1825
	60	60.00			χ^2=1.0112

For degrees of freedom $k=8-2=6$ and confidence interval *95%* ($\alpha=0.05$) is: $\chi_{0.05}^2 = 12.60$

7. CONCLUSION

For open gears the following conclusions under presented operation conditions can be drawn from the results presented above:

- Reliability of open gears were found to be affected by both NLGI consistency number and type of lubricating grease.
- Increasing the NLGI consistency number of these lubricating greases tended to reduce the failure rate and led to a longer open gears life.
- The lithium lubricating grease with EP additives ISO-L-XCCEB gives a longer life compared with the case without EP additives ISO-L-XCCDA.
- The lubricating grease ISO-L.XCFHB NLGI 3 gives the longest life among all the lubricating greases studied in the present work.

The paper presented the following:

- The analysis of the kinds of lubricating greases for open gears.
- The flowchart for the selection of the lubricating grease in function of all relevant influential factors.
- The reliability curves as a function of tribological properties of lubricating greases under presented operating conditions of investigation.

REFERENCES

[1.] *Alliston - Greiner A.F.*, **Testing Extreme Pressure and Anti-Wear Performance of Gear Lubricants**, Proc.Inst.Mech.Eng., Vol. 205, 1991, pp. 89-101

[2.] *Jost P.H.*, **Modern Tribology, past and future**, Proceedings Int. Congress on Tribology, Budapest, Hungary, 1993, Vol.6. pp.1-36.

[3.] *Dowson D., Higginson G.R.*, **Elastohydrodynamic Lubrication**, Pergamon Press, Oxford, 1966.

[4.] *Hamrock B.J.*, **Elastohydrodynamic Lubrication of Elliptical Contacts**, Proceedings of the 1st Symposium "Intertribo '81 ", High Tatras, Czechoslovakia, 1981, pp.6-16.

[5.] *Cheng H.S.*, **"Elastohydrodynamics and Failure Prediction "**, Lubrication Science, 1990, Vol.2, No.2, pp. 133-156.

[6.] *Shuchun L, Zongi L.*, **A Numerical Solution for Elastohydrodynamic Lubrication Film Thickness of Involute Spur Gear and its Application of Gear Industries"**, Proceedings of 11th Int. Conference on Production Research, Hefei, 1991, pp. 1037-1039.

[7.] ISO 6743 / 6 , Classification of Lubricants, Industrial Oils and related products (class L), part 6, Family C (Gears), 1989.

[8.] Lubricants, industrial oil and related products (class L) - Recommendation for the choice of lubricants for machine tools, ISO Technical Report 3498, 1986.

[9.] Lubricants, industrial oil and related products (class l)- Classification part 9, Family X (greases), ISO- International Standard 6743-9, 1987.

[10.] *Rakic R.*, **"Die Zuverlässigkeit von Zahnradgetrieben in Abhängigkeit von tribologischen Schmierstoffeigenschaften"**, Tagung Zahnradgetriebe, Dresden, Vortragungsband, 1989, 462-467.

[11.] *Rakic R.*, **The Effect of Tribological Properties of Lubricants on Reliability of Gears** , Proceedings of Int. Scientific Conference on Trends in Agricultural Engineering,, Prague, Supplement, 1992, pp.68-73.

[12.] *Rakic R.*, **The Influence of Tribological Properties of Lubricants on the Tribomechanical System Elements in Nonconformal Contact**, Proceedings of the 6th Int. Congress in Tribology Eurotrib'93, Budapest, 1993, Vol.2.pp.228-233.

[13.] *Rakic R.*, **The Influence of Lubricant on Tribological Behaviour of Gears**, Proceedings of the 6th Int. Symposium Intertribo'96, the High Tatras, 1996, pp. 160- 163.